**TECHNICAL UNIVERSITY OF LIBEREC**
**Faculty of Science, Humanities
and Education**

# Numerical Modelling of Heat Phenomena Induced by Heat Radiation

*Roman Knobloch*

# DOCTORAL THESIS

*Department of Mathematics and Didactics of Mathematics*
Supervisor: *Assoc. Prof. Jaroslav Mlýnek*

I declare that I carried out this doctoral thesis independently and using only the cited articles, books, and other professional sources.

In Liberec, April 24, 2019

# Contents

# Mathematical Notation

| Symbol | Meaning/Page |
|--------|--------------|
| $A$ | linear operator |
| $B$ | nonlinear operator |
| $C^k(\Omega)$ | space of $k$-times continuously differentiable functions defined on $\Omega \subset \mathbb{R}^d$ |
| $u, v$ | vector as an element of a linear vector space |
| $X, Y$ | Banach space |
| $V$ | Hilbert space |
| $f$ | linear functional defined on Hilbert space $V$ |
| $p, P$ | probability |
| $B_d$ | ball in the $d$-dimensional Euclidean space |
| $EX$ | expected value of a random quantity $X$ |
| $DX$ | variance of a random quantity $X$ |
| $F(x)$ | cost function with multidimensional variable $x$ |
| $V_d(R)$ | volume of a ball with radius $R$ in the $d$-dimensional Euclidean space |
| $S_d(R)$ | surface of a ball with radius $R$ in the $d$-dimensional Euclidean space |
| $\Gamma(n)$ | gamma function value for a natural number $n$ |
| $n!$ | factorial of a natural number $n$ |
| $n!!$ | double factorial of a natural number $n$ |
| $NP$ | number of individuals in a generation of a differential evolution algorithm |
| $NG$ | number of generations of a differential evolution algorithm |
| $G$ | generation number |
| $G(k)$, $k = 0, 1, 2, \ldots$ | $k$-th generation of a differential evolution algorithm |

| | |
|---|---|
| $D$ | dimension of an optimization task, number of variables |
| $CR$ | crossover probability |
| $F$ | mutation factor |
| $R$ | parameter in a modified differential evolution algorithm (MDEA) that specifies the ratio of random individuals that are replaced by random individuals |
| $\mathbb{R}^d$ | $d$-dimensional Euclidean space |
| $S$ | search space – the domain of the cost function |
| $S^*$ | solution set, set containing global minima of the cost function $F(x)$ |
| $S_\varepsilon^*$ | optimal solution set |
| $\mu(S)$ | measure of the search space $S$ |
| $L$ | Lipschitz constant |
| $\mathrm{dist}(x_1, x_2)$ | distance of points $x_1$, $x_2$ |
| $\Delta f$ | Laplace operator applied on the function $f$ |
| $\lfloor x \rfloor$ | lower integer part of number $x$ |
| $\lceil x \rceil$ | upper integer part of number $x$ |
| $d$ | dimension of a Euclidean space |
| $\alpha_\mathrm{S}$ | significance level |
| $C_\mathrm{R}$ | relative certainty |

# Physical Notation

| Symbol | Meaning/Page | Unit |
|--------|--------------|------|
| $\alpha$ | coefficient of the heat transfer between a material body and air | $W/(m^2 \cdot K)$ |
| $\alpha_r$ | coefficient of radiation absorption | 1 |
| $c$ | material specific heat | $J/(kg \cdot K)$ |
| $c_0$ | speed of light in vacuum | $c_0 = 2.998 \cdot 10^8\,m/s$ |
| $\varepsilon_r$ | radiation emissivity | 1 |
| $F_{dev}$ | deviation function – function quantifying the deviation of radiation intensity on the mould surface from the recommended intensity $I_{rec}$ | |
| $h$ | Planck constant | $h = 6.626 \cdot 10^{-34}\,Js$ |
| $I$ | intensity of the heat radiation | $W/m^2$ |
| $I_j$ | total radiation intensity incident on the $j$-th elementary surface from all heaters | $W/m^2$ |
| $I_{jl}$ | heat radiation intensity generated by the $l$-th heater incident on the $j$-th elementary surface | $W/m^2$ |
| $I_{rec}$ | recommended radiation intensity on the mould surface | $W/m^2$ |
| $j$ | power radiated from a unit surface | $W/m^2$ |
| $k_B$ | Boltzmann constant | $k_B = 1.381 \cdot 10^{-23}\,JK^{-1}$ |
| $\hat{\lambda}$ | tensor of heat conductivity | $W/(m \cdot K)$ |
| $\lambda$ | heat conductivity | $W/(m \cdot K)$ |
| $\Lambda$ | thermal conductivity | $m^2/s$ |

| | | |
|---|---|---|
| $\rho$ | density | kg/m$^3$ |
| $\rho_\mathrm{r}$ | coefficient of radiation reflectivity | 1 |
| $Q$ | density of volume heat sources | W/m$^3$ |
| $\sigma$ | Stefan–Boltzmann constant | $\sigma = 5.67 \cdot 10^{-8}\,\mathrm{Wm^{-2}K^{-4}}$ |
| $t$ | time | s |
| $T$ | temperature | K, °C |
| $\tau_\mathrm{r}$ | coefficient of radiation transmissivity | 1 |

# Chapter 1

# Introduction

The subject matter of this thesis consists in principle of two main parts that are closely interconnected. The first part deals with an optimization technique used to optimize heating of a shell metal mould by a set of infrared heaters. The target of the optimization is to achieve a uniform field of heat flux that guarantees the technologically given temperature range for the whole mould body. Finally, the method of differential evolution algorithm proved itself most suitable for this task.

Nevertheless, during the work on the project it became apparent that even the classic differential evolution algorithm has its intrinsic limits regarding the ability to guarantee the convergence to the global minimum of the cost function. We found out that a principal weakness of the classic differential evolution algorithm is its tendency to premature convergence to the local minimum of the cost function.

This fact was a starting point for a pursuit of an improvement of the classic differential evolution algorithm that could provide better results regarding the global convergence. The modified differential evolution algorithm is the result of these aspirations. The modified algorithm brings substantial improvement not only from theoretical but also from practical point of view.

As far as the theory is concerned, we were able to prove for the modified algorithm the ability to converge to the global minimum of the cost function in asymptotic sense. From the practical point of view this means that the algorithm is immune to the premature convergence. That is the generations of the algorithm do not stagnate around a local minimum of the cost function. This potential stagnation is a principal weakness of the classic differential evolution algorithm.

Substantial energy was also invested in the effort to extract some usable information from the situation when even the modified differential evolution algorithm does not find any improvement in seeking for the global minimum of the cost function. Since the full theoretical analysis of the differential evolution analysis is not available at this stage, we concentrated primarily on the role of random individuals in the convergence process. We present several statements in this field that make it possible to interpret quantitatively this negative result.

The second part of the thesis is focused on the task to utilize the optimized heat flux as an input quantity in the process of modelling the temperature field inside the mould and in particular on the mould working surface. Here, the starting point is represented by the heat equation together with boundary and initial conditions. Since the infrared heating of the mould is used, we can hardly neglect the own heat radiation of the mould itself in the numerical calculation. This own radiation is described quantitatively by Stefan–Boltzmann law.

The doctoral thesis is divided into eight chapters. Following this introduction, the second chapter (Motivation) provides the reasons for research in the area of infrared heating and other important circumstances and connections of the investigated topics.

The third chapter (Mathematical Background) summarizes some mathematical prerequisites that are used in the following text. The fourth chapter (Radiation Heating Model) describes the theoretical models that are used to represent real infrared heaters and shell metal moulds. It also provides a brief account how the radiation heat flux is calculated on the mould surface. Additionally, it introduces the cost function that evaluates the uniformity of the heat flux on the heated surface of the mould.

The fifth chapter (Optimization of the Heat Flux Distribution) starts with a brief account of evolutionary computing methods. Then it provides a thorough description of the classic differential algorithm including the counterexamples to its global convergence. Then, the modified differential evolution algorithm is introduced. For the modified differential evolution algorithm it is possible to prove the convergence to the global minimum of the cost function in asymptotic sense using relatively weak assumptions. Subsequently, the role of random individuals in the operation of modified differential evolution algorithm is examined.

The chapter six (Models of Heat Conduction) describes the heat equation including the boundary and initial conditions and methods leading to the weak solution of this heat equation.

The chapter seven (Numerical Results) provides an account of specific methods and techniques used to find a solution of the practical task. The task consists in the optimization of a set of 16 infrared heaters over a test mould. The first stage of the task is focused on the optimization leading to a uniform heat flux field on the heated surface of the mould. The second stage is concentrated on modelling of the temperature field in the mould including the numerical results.

The chapter eight (Conclusions) provides a brief summary of considerable findings and relevant results the author achieved during the work on the doctoral thesis project.

# Chapter 2

# Motivation

Heating of bodies is relatively frequent in technical practice. It mostly takes part in technological procedures when a given material or a semiproduct has to be processed at a technologically given temperature. In this thesis we concentrate specifically on the method of radiation heating. The radiation heating is realized by a set of infrared heaters that are suitably positioned over the heated body.

As far as the heated bodies are concerned we concentrate on shell metal moulds. By a shell mould we mean a body in the three dimensional Euclidean space whose thickness is relatively small compared to its length and width. Instances of two shell moulds used in the real production are given in Figure 2.1.

Such shell moulds are used in the automotive industry in the production of a plastic imitation of leather. The plastic imitation of leather, hereinafter referred to as plastic leather, serves for surfacing of some parts of cars interiors that potentially come into contact with driver's or passenger's body. The usual examples where the plastic leather is used are dash boards, doors fillings and elbow supports. The purpose of the plastic leather is to improve the surface properties of hard plastic parts and to contribute to better overall impression from the car interior. The technology of the plastic leather production is called the Slush Moulding.

The Slush Moulding Technology consists in the following procedure: A relatively large shell metal mould of possibly complicated shape is preheated to a required temperature. Subsequently, powder of polyethylene, polyurethane or PVC is sprinkled evenly over the working side of the mould, that is over the side where the plastic leather is formed. The high temperature causes gradual sintering of the plastic powder that constitutes the base of the plastic leather. At the
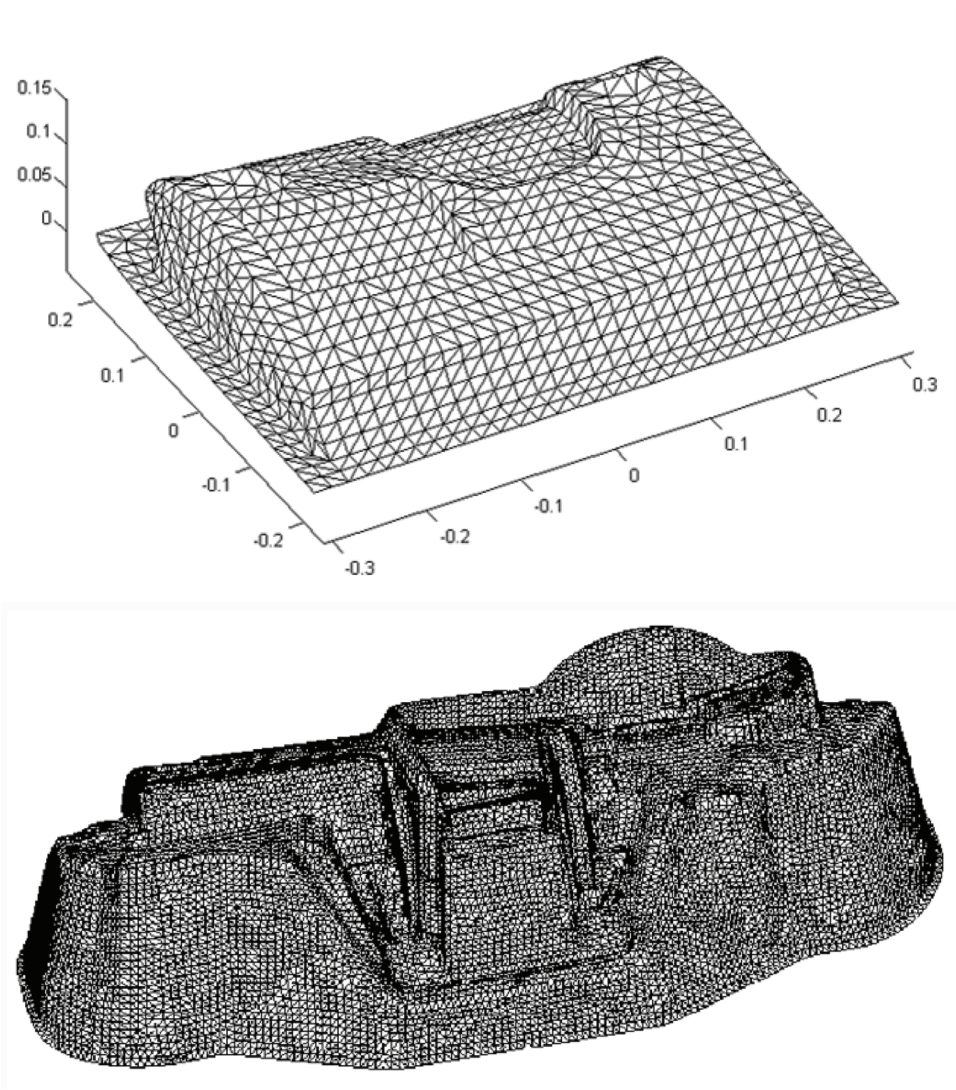
Figure 2.1: Examples of shell moulds used in the Slush Moulding Technology

same time more plastic powder is added which leads to the increase in thickness of the plastic layer. Simultaneously, the mould is heated to keep the technological temperature of the mould stable. After the thickness of the plastic leather achieves the required value (approximately after three minutes), the whole mould is cooled down by cold water and the plastic leather is carefully detached from the mould.

In principle, the heating of the mould can be realized by several different procedures. The reasonable alternatives are heating by hot air, hot oil or hot sand, and heating by infrared heaters. The infrared heating uses no auxiliary medium that would be necessary to heat up (air, oil or sand), which is the base for better energy efficiency of the infrared heating (by approximately 30%). Additionally, it is possible to switch off and on selectively a part of the heaters which contributes to higher flexibility of the heating. The high cleanness of the infrared heating when compared with the other alternative heating techniques is an important advantage as well.

The infrared heating is realized by a set of several up to several tens of standard infrared heaters. The number and heating power of heaters depend on the size and complexity of the mould. The heaters radiate on the heated side of the mould (the side where the plastic leather is not formed). Examples of infrared heaters are given in Figures 2.2 and 2.3.



Figure 2.2: Infrared heater Phillips with nominal power 1000 W

The incident heat flux gradually raises the temperature on the heated side and subsequently in the whole body of the mould. The achievement of the proper technological temperature and also the uniformity of the temperature field on the whole working side of the mould (where the plastic leather is formed) is a
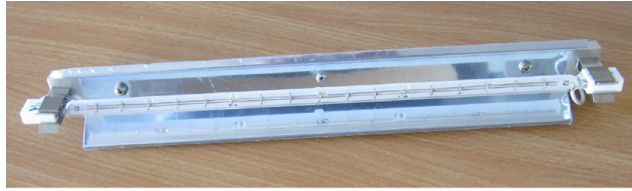
Figure 2.3: Infrared heater Ushio with nominal power 2000 W

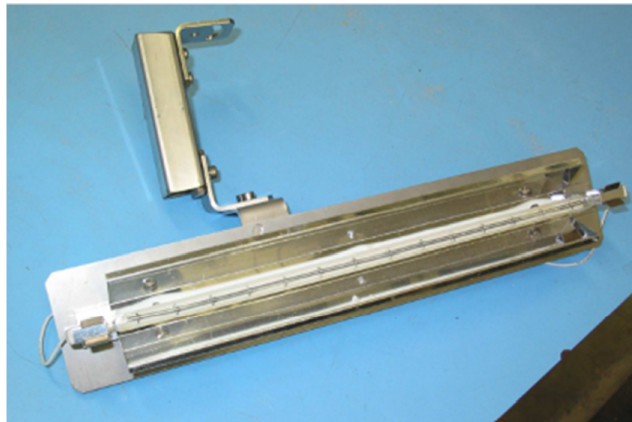necessary prerequisite for production of high quality plastic leather with perfect surface structure and even colour shade. In real production conditions it is hardly possible to attain fully the exact temperature and thoroughly uniform temperature field, but it is possible to come relatively close to the ideal conditions. The real target is thus the state when the average temperature on the working side of the mould achieves approximately the required technological value and the differences between the real and average temperature do not exceed the technologically set limits. This target is attained by a suitable positioning of a set of infrared heaters over the surface of the heated side of the mould.

The reasons that complicate the achievement of the uniform temperature field are primarily:

– shape complexity of the heated mould,

– time limits ensuing from requirements for high production productivity and cost effectiveness,

– energy consumption limits; in principle, the uniformity of the temperature field can often be improved by increasing the number of infrared heaters, but this leads to higher energy consumption.

In the real production the infrared heaters are mostly set by a try and error procedure. This means that qualified technicians guess suitable positions for infrared heaters over the mould. Then a test heating takes place. If the temperature field on the working side of the mould attains the required level and uniformity, then this setting is considered acceptable and it is subsequently used in the Slush Moulding Technology. Otherwise, corrections of heaters positions and orientations have to be made and the temperature field is again thoroughly monitored during another test heating. These procedures are repeated until the temperature field on the working side of the mould surface has the required temperature level and uniformity. This manual approach is tedious and time consuming. It usually

takes from one to three weeks depending on the mould dimensions, its complexity and the number of heaters. Additionally, such a setting is not accurate and it is not obvious how to quantify the quality of the specific setting.

We can summarize that the manual positioning of infrared heaters has the following principle disadvantages:

– the dependence of the temperature field on the qualifications and practical experience of the competent technicians,

– long times necessary for the adequate setting,

– the quality of the manual setting is not certain and besides it is hardly quantifiable.

In order to simplify and accelerate the procedure of finding suitable positions of infrared heaters over the mould the authors of article [33] created a simulation programme in software environment IREviewBlender in cooperation between the Technical University of Liberec and company LENAM. This software tool makes it possible to simulate graphically on a computer the setting of individual infrared heaters providing simultaneously the corresponding total intensity of the heat radiation incident on the mould surface. This simulation programme does not optimize the heaters setting in any way, it only visualizes the resulting intensity of the heat flux. The programme is described thoroughly in the article [33].

Another attempt in this field is a programme modelling the heating radiation intensity field in the space region around infrared heaters considering their specific technical parameters. For details see [15].

The developed software tools mentioned above provide useful auxiliary implementations to be utilized during the infrared heaters setting in the production. Nevertheless, up to now no real practical method optimizing the infrared heaters positioning has been available.

It is preferable to have theoretically based and quantifiable procedure for the setting of infrared heaters over the mould. That is why we used a different approach proposed by the doctoral thesis supervisor. This approach uses the fact that the heat radiation intensity is an additive quantity. This means that the total heat radiation can be calculated as a sum of intensities generated by individual heaters for each part of the mould. Besides, the producer of plastic leather can provide the recommended heat intensity $I_{\mathrm{rec}}$ that should be used for

the heating. In these circumstances the task to find the optimal infrared heaters setting can be reformulated as an optimization task.

This optimization task can be solved by various optimization techniques. Nevertheless, due to complexity of the cost function the standard optimization techniques (e.g. gradient methods) fail to provide usable results. We tested several other alternative optimization techniques. Finally, differential evolution algorithms and in particular the modified differential evolution algorithm proposed by the author proved best as a feasible optimization tool. The results received by the original classic differential evolution algorithm are summarized in articles [27], [28], [29], and [30]. The modified differential evolution algorithm, its properties and comparison to the classic differential evolution algorithm were extensively studied. The connected findings and results are described in articles [12], [13], [14], and [23].

Since the quality of the produced plastic leather is strongly dependent on the temperature on the working side of the mould it is important to have a detailed information on the temperature field in the mould. In the real production the temperature field is monitored by temperature sensors at several up to several tens of points on the surface of the mould during the test heating. There exist several standard methods how to measure the temperature of the mould:

- Measuring by thermocouples

- Measuring based on electrical resistance change with temperature (resistance sensors, termistors)

- Measuring based on dependence of electromagnetic waves radiated by hot bodies on temperature (infrared detectors, pyrometers)

Although temperature measurements are frequently used their proper experimental arrangement is relatively demanding and costly. Besides, some methods of temperature monitoring affect negatively either the temperature field or the production technology. Further, the deviations in the measured temperatures are sometimes relatively significant inducing uncertainty in the temperature field and its uniformity. For details on temperature measuring and temperature monitoring experimental arrangements see [31].

This is the reason to try to replace the experimental temperature measuring by modelling the temperature field virtually by means of a computer. We use the

programme package ANSYS that makes possible to calculate the temperature field on the basis of known heat sources and material parameters of the mould. Of course also the boundary conditions play an important role in the temperature field modelling. This procedure makes possible to calculate and depict the temperature field in the mould in a suitable way and to check it against the technological temperature requirements ensuing from the plastic leather production. The results of the temperature field modelling are described and summarized in articles [22], [24], [25], and [26].

On the assumption that a uniform temperature field is generated by a uniform infrared heating (such an assumption is not self-evident and it should be properly motivated), we can divide the modelling of the temperature field into two relatively independent parts:

1. The heating optimization

   The optimization task that provides the infrared heaters positioning over the mould and the radiation heat flux incident onto the heated side of the mould.

2. The temperature field modelling

   The numerical calculation of the temperature field generated by the uniform heating considering proper boundary and initial conditions and its comparison with the target state (comparing it with the target temperature range and analyzing of the uniformity of the temperature field).

With respect to the fact that the infrared heaters have a relatively complex heat radiation diagram (a scheme describing the directional dependence of the heat radiation distribution in the neigbourhood of the heater), it is not possible to optimize only the positions of the heaters but it is essential to optimize their space orientation as well.

The temperature field modelling is on the other hand a construction of a solution of a specific partial differential equation (the heat equation) with boundary and initial conditions. The optimized heat flux is here used as a heat source modifying the boundary condition on the heated side of the mould. The method of finite elements and software package ANSYS are used for the numerical calculations of the temperature field in the mould.

# Chapter 3

# Mathematical Background

In this chapter we summarize the mathematical concepts and statements that have a relation to the topics and models described in the following parts.

## 3.1  Summary of Linear Functional Analysis

In this section we briefly summarize some definitions and statements from the area of functional analysis and partial differential equations. We suppose that the reader is familiar with the following general concepts: vector space, scalar product, norms on vector spaces, Banach space and Hilbert space. The below mentioned concepts are in full detail introduced and motivated in books [10], [18], [19], [20], and [43].

### 3.1.1  Linear Operators on Banach Spaces

The theory of operators on Banach and Hilbert spaces is a general tool used in the theory of partial differential equations. First we recapitulate some definitions.

**Definition 3.1.1.** *Let $X$ and $Y$ be Banach spaces. We say that $A$ is a linear operator from $X$ into $Y$ if*

$$A(u + v) = A(u) + A(v)$$

*and*

$$A(\alpha u) = \alpha A(u)$$

*for all $u, v \in X$ and for all $\alpha \in \mathbb{R}$.*

**Definition 3.1.2.** *Let $X$ and $Y$ be Banach spaces with norms $\|\cdot\|_X$ and $\|\cdot\|_Y$, respectively. We say that a linear operator $A$ is continuous if there exists a constant $C > 0$ such that*

$$\|A(u)\|_Y \leq C\|u\|_X \quad \forall u \in X.$$

The relation between operator linearity and continuity is straightforward in Banach spaces of finite dimension. In this case each linear operator is continuous. In general, this is not the case for Banach spaces of infinite dimension.

**Proposition 3.1.1.** *Let $X$ and $Y$ be Banach spaces. If the space $X$ is of finite dimension then each linear operator $A : X \to Y$ is continuous.*

Based on Definition 3.1.2 we can define a norm for continuous operators.

**Definition 3.1.3.** *Let $A : X \to Y$ be a continuous operator from a normed space $X$ into a normed space $Y$. Then*

$$\|A\| = \inf\{C \geq 0 : \|A(u)\|_Y \leq C\|u\|_X\} \quad \forall u \in X.$$

**Remark 3.1.1.** *The infimum in the previous definition is attained as the set of all such $C$ is closed, nonempty, and bounded from below.*

A linear operator whose values are real numbers (scalars) is called a linear form or a linear functional.

**Theorem 3.1.2** (Riesz)**.** *Let $V$ be a Hilbert space with a scalar product $(\cdot, \cdot)_V$. Then for each linear continuous functional $f$ defined on $V$ there exists a unique element $u \in V$ such that*

$$f(v) = (u, v)_V \quad \forall v \in V.$$

## 3.1.2 Bilinear Forms and Lax–Milgram Lemma

Let us remind that a scalar mapping $a(\cdot, \cdot)$ defined on $V \times V$, where $V$ is a linear vector space is a bilinear form if for each fixed $v \in V$ the mappings $a(\cdot, v)$ and $a(v, \cdot)$ are linear.

**Definition 3.1.4.** *We say that the bilinear form $a(\cdot, \cdot)$ is continuous if there exists a constant $C_1 > 0$ such that*

$$|a(u, v)| \leq C_1 \|u\|_V \|v\|_V \quad \forall u, v \in V.$$

**Lemma 3.1.3** (Lax-Milgram). *Let $V$ be a Hilbert space and let $a(\cdot, \cdot)$ be a continuous bilinear form for which there exists a constant $C_2 > 0$ such that*

$$|a(u, u)| \geq C_2 \|u\|^2 \quad \forall u \in V. \tag{3.1}$$

*Then for each linear continuous functional $f$ defined on $V$ there exists a unique element $u \in V$ such that*

$$a(u, v) = F(v) \quad \forall v \in V. \tag{3.2}$$

The property defined by the relation (3.1) is called $V$-ellipticity.

**Definition 3.1.5.** *The bilinear form $a(\cdot, \cdot)$ defined on $V \times V$, where $V$ is a linear vector space is called symmetric if*

$$a(u, v) = a(v, u) \quad \forall u, v \in V.$$

Under the assumption that the bilinear form is symmetric and nonnegative the Lax-Milgram lemma can be reformulated as the following theorem.

**Theorem 3.1.4.** *Let the assumptions of the Lax-Milgram lemma be satisfied. Let additionally the bilinear form $a(\cdot, \cdot)$ be symmetric and $a(v, v) \geq 0$ for all $v \in V$. Then the problem (3.2) is equivalent to the task: Find $u \in V$ such that*

$$J(u) = \inf_{v \in V} J(v),$$

*where $J$ is a quadratic functional given by the formula*

$$J(v) = \frac{1}{2}a(v, v) - f(v), \quad v \in V.$$

### 3.1.3   Sobolev Spaces and Integral Identities

The solutions of many problems described by partial differential equations are looked for in special function spaces called Sobolev spaces. We have to limit in a suitable way the domains on which the above mentioned problems are solved. We consider the Sobolev spaces defined exclusively on bounded regions with Lipschitz continuous boundaries. Such domains form a reasonably wide class of regions for practical tasks. Additionally, such domains embody the property that the outer normal is defined almost everywhere, which is important for concepts such as normal derivatives or normal components of some quantities.

**Definition 3.1.6.** *A bounded domain $\Omega \subset \mathbb{R}^d$ is said to have a Lipschitz continuous boundary if for any $x \in \Gamma = \partial\Omega$ there exists a neighbourhood $U = U(x)$ such that the set $U \cap \Omega$ can be expressed, in a Cartesian coordinate system $(x_1, \ldots, x_d)$, by the inequality $x_d < F(x_1, \ldots, x_{d-1})$, where $F$ is a Lipschitz continuous function. We denote by the symbol $\mathcal{L}$ the set of all bounded domains with Lipschitz continuous boundary.*

From now on we consider only domains $\Omega \subset \mathbb{R}^d$ with Lipschitz continuous boundaries. That is $\Omega \in \mathcal{L}$.

We also need a concept of the weak derivative. For any $v \in C^\infty(\bar{\Omega})$ and the multiindex $m = (m_1, \ldots, m_d)$ we define the classical $m$-th derivative

$$D^m v = \frac{\partial^{|m|} v}{\partial x_1^{m_1} \cdots \partial x_d^{m_d}} ,$$

where $m_1, \ldots, m_d$ are nonnegative integers and

$$|m| = m_1 + \ldots + m_d.$$

We say that a function $v \in L^2(\Omega)$ has the $m$-th weak derivative in $L^2(\Omega)$ if there exists a function $z \in L^2(\Omega)$ such that

$$\int_\Omega zw \, \mathrm{d}x = (-1)^{|m|} \int_\Omega v D^m w \, \mathrm{d}x \quad \forall w \in C^\infty(\Omega).$$

The function $z$ is called the $m$-th weak derivative of $v$ and we set $D^m v = z$.

Now, we can define Sobolev spaces in the following way. For $k = 0, 1, \ldots$ the Sobolev space $H^k(\Omega)$ is defined as

$$H^k(\Omega) = \{v \in L^2(\Omega) : D^m v \in L^2(\Omega), \ |m| \leq k\}.$$

The Sobolev space $H^k(\Omega)$ equipped with scalar product

$$(v, w)_{k,\Omega} = \sum_{|m| \leq k} \int_\Omega D^m v D^m w \, \mathrm{d}x \quad \forall v, w \in H^k(\Omega),$$

is a Hilbert space.

We further introduce the induced norm

$$\|v\|_{k,\Omega} = \left( \sum_{|m| \leq k} \int_\Omega |D^m v|^2 \, \mathrm{d}x \right)^{\frac{1}{2}} \quad \forall v \in H^k(\Omega),$$

and the seminorm

$$|v|_{k,\Omega} = \left( \sum_{|m|=k} \int_\Omega |D^m v|^2 \, \mathrm{d}x \right)^{\frac{1}{2}} \quad \forall v \in H^k(\Omega).$$

Weak formulations of tasks involving partial differential equations are derived by means of Green's theorems. The first Green theorem can be expressed in the following way(see [19] or [36]) .

**Theorem 3.1.5.** *Let $\Omega \subset \mathbb{R}^d$ be a bounded domain with Lipschitz continuous boundary, $\Omega \in \mathcal{L}$. Then for each $i \in \{1, \ldots, d\}$ the following equality holds*

$$\int_\Omega \frac{\partial u}{\partial x_i} v \, \mathrm{d}x + \int_\Omega u \frac{\partial v}{\partial x_i} \, \mathrm{d}x = \int_{\partial\Omega} n_i u v \, \mathrm{d}S$$

*for all $u, v \in H^1(\Omega)$. Here $n_i$ stands for the corresponding component of the outer normal $n$.*
*The integral identity can also be expressed in the vector form*

$$\int_\Omega (\nabla u) v \, \mathrm{d}x + \int_\Omega u (\nabla v) \, \mathrm{d}x = \int_{\partial\Omega} u v \boldsymbol{n} \, \mathrm{d}S. \tag{3.3}$$

The second Green's theorem can be formulated in the following way (see [4] or [6]).

**Theorem 3.1.6.** *Let $\Omega \subset \mathbb{R}^d$ be a bounded domain with Lipschitz continuous boundary, $\Omega \in \mathcal{L}$. Let $u \in C^2(\Omega)$, $v \in C^1(\Omega)$, where $C^k(\Omega)$ denotes the space of $k$-times continuously differentiable functions defined on $\bar\Omega$. Then*

$$\int_\Omega (\Delta u) v \, \mathrm{d}V = \int_{\partial\Omega} \frac{\partial u}{\partial n} v \, \mathrm{d}S - \int_\Omega \nabla u \cdot \nabla v \, \mathrm{d}V,$$

*where the symbol $\frac{\partial u}{\partial n}$ denotes the derivative of the function $u$ with respect to the outer normal $n$.*

**Proof:** The proof of the statement follows easily from the theorem of Gauss–Ostrogradski. We can write the integral identity of Gauss–Ostrogradski in the following vector form

$$\int_\Omega \nabla \cdot \boldsymbol{F} \, \mathrm{d}V = \int_{\partial\Omega} \boldsymbol{F} \cdot \boldsymbol{n} \, \mathrm{d}S,$$

where $\boldsymbol{F}$ is a differentiable vector field.

Next, we use the obvious differential identity

$$\nabla \cdot (v\boldsymbol{G}) = \nabla v \cdot \boldsymbol{G} + v\nabla \cdot \boldsymbol{G},$$

which holds for any differentiable scalar field $v$ and differentiable vector field $\boldsymbol{G}$ and get

$$\int_\Omega \nabla v \cdot \boldsymbol{G} \, \mathrm{d}V + \int_\Omega v\nabla \cdot \boldsymbol{G} \, \mathrm{d}V = \int_\Gamma v\boldsymbol{G} \cdot \boldsymbol{n} \, \mathrm{d}S.$$

By putting $\boldsymbol{G} = \nabla u$ we obtain

$$\int_\Omega \nabla v \cdot \nabla u \, \mathrm{d}V + \int_\Omega v\nabla \cdot \nabla u \, \mathrm{d}V = \int_\Gamma v\nabla u \cdot \boldsymbol{n} \, \mathrm{d}S.$$

Because $\nabla \cdot \nabla u = \Delta u$ and $\nabla u \cdot \boldsymbol{n} = \frac{\partial u}{\partial n}$, we finally get

$$\int_\Omega (\Delta u)v \, \mathrm{d}V = \int_{\partial\Omega} \frac{\partial u}{\partial n}v \, \mathrm{d}S - \int_\Omega \nabla u \cdot \nabla v \, \mathrm{d}V,$$

which was to prove.

$\square$

### 3.1.4 Function Spaces for Nonstationary Problems

Nonstationary evolution problems require the construction of function spaces that include a time variable. The introduced concepts are inspired primarily by books [4] and [37].

We consider a function $u(x,t)$ with $x \in \Omega$, $\Omega \in \mathcal{L}$, and $t \in \langle 0,\tau \rangle$, $\tau \in (0,\infty)$ and assume that for all or almost all $t$ the function $u(x,t)$ belongs to a suitable Hilbert space $V$ (for instance $H^1(\Omega)$). The meaning of this assumption is a sort of separation of space and time variables and is motivated by the fact that the requirements laid on space and time variables are usually different.

Then we can consider $u$ as a generalized function of a real variable $t$ with values in the function space $V$

$$u : \langle 0,\tau \rangle \to V.$$

This means that we can further on use the notation $u(t)$, $\dot{u}(t)$ instead of $u(x,t)$ and $\frac{\partial}{\partial t}u(x,t)$. Since we deal with evolution tasks containing the time derivative of the solution, we have to introduce the concept of integration of the generalized functions $u(t)$, $\dot{u}(t)$.

The standard procedure is to use the concept of measurability and then to define the integral. First we introduce the set of simple functions $s : \langle 0, \tau \rangle \to V$ such that they attain only a finite number of values. They can be written as

$$s(t) = \sum_{j=1}^{n} \chi_{E_j}(t) u_j, \quad 0 \le t \le \tau, \tag{3.4}$$

where $u_1, \ldots, u_n \in V$ and $E_1, \ldots, E_n$ are measurable mutually disjoint subsets of $\langle 0, \tau \rangle$. The function $\chi_{E_j}(t)$ is a characteristic function of the set $E_j$.

We say that $f : \langle 0, \tau \rangle \to V$ is measurable if there exists a sequence of simple functions $s_k : \langle 0, \tau \rangle \to V$ such that for $k \to \infty$ we have

$$\| s_k(t) - f(t) \|_V \to 0 \quad \text{for almost all} \quad t \in \langle 0, \tau \rangle.$$

The integral is defined first for simple functions. If $s$ is given by the relation (3.4), we define

$$\int_0^\tau s(t)\,\mathrm{d}t = \sum_{j=1}^{n} |E_j| u_j.$$

For a generalized function $f : \langle 0, \tau \rangle \to V$ we can introduce the integral in the following way.

**Definition 3.1.7.** *We say that the function $f : \langle 0, \tau \rangle \to V$ is integrable on $\langle 0, \tau \rangle$ if there exists a sequence of simple functions $s_k : \langle 0, \tau \rangle \to V$ such that*

$$\int_0^\tau \| s_k(t) - f(t) \|_V \,\mathrm{d}t \to 0 \quad \text{for} \quad k \to \infty.$$

It is possible to verify that $\{ s_k(t) \}$ is a Cauchy sequence, so that the limit in the definition above is properly defined and does not depend on the specific selection of the sequence $\{ s_k(t) \}$.

Then the following statement is valid.

**Proposition 3.1.7.** *The measurale function $f : \langle 0, \tau \rangle \to V$ is integrable on $\langle 0, \tau \rangle$ if the real function $t \to \| f(t) \|_V$ is integrable on $\langle 0, \tau \rangle$. Additionally, it holds*

$$\left\| \int_0^\tau f(t)\,\mathrm{d}t \right\| \le \int_0^\tau \| f(t) \|_V \,\mathrm{d}t \quad \text{and}$$

$$\left( u, \int_0^\tau f(t)\,\mathrm{d}t \right)_V = \int_0^\tau (u, f(t))_V \,\mathrm{d}t \quad \forall u \in V.$$

## 3.2  Elementary Statistics

In this section we present several concepts from the theory of mathematical statistics that will be necessary in Section 5.7.

### 3.2.1  Simple Probabilities

We will need probabilistic estimates dealing with random points from the cost function domain. These estimates can be based on the concept of geometric probability (as introduced in the book [50], page 56) and elementary calculus.

We can formulate the following problem: We have a domain $D$ with the total volume $V$ that is divided into $m$ parts of equal volume $v$. We choose one of these parts as target and then generate the same number $m$ of random points from the domain $D$. The question is what is the probability that we hit the target region at least once.

Since the volumes of individual parts are equal, the probability to hit specific regions are also equal. Let us denote the probability to hit a specific region with one random point as $p$. It clearly holds

$$p = \frac{1}{m} = \frac{v}{V}.$$

The probability to hit the target region at least once generating $m$ random points is

$$P(m) = 1 - \left(1 - \frac{1}{m}\right)^m.$$

Let us take a closer look at the sequence

$$\alpha_m = \left(1 - \frac{1}{m}\right)^m = \frac{1}{\left(1 + \frac{1}{m-1}\right)^m}.$$

From elementary analysis it is clear that the sequence $\alpha_m$ is increasing with a limit

$$\lim_{m \to \infty} \alpha_m = \frac{1}{e}.$$

The probability $P(m)$ then forms a decreasing sequence with a limit

$$\lim_{m \to \infty} P(m) = 1 - \frac{1}{e}.$$

But that obviously indicates that the number $1 - \frac{1}{e}$ represents a lower estimate of the probability $P(m)$.

This probability estimate works analogously also for different numbers of random points $n$. Let us now evaluate the probability of hitting the target region using $n$ random points. For the sake of simplicity we denote

$$n = \chi \cdot m.$$

Here the number $\chi$ is a factor specifying the ratio between the actual number of random points $n$ and the number of regions $m$.

Then the probability $P(m, n)$ that we hit the target region at least once is

$$P(m,n) = 1 - \left(1 - \frac{1}{m}\right)^n = 1 - \left(1 - \frac{1}{m}\right)^{\chi m} = 1 - \left[\left(1 - \frac{1}{m}\right)^m\right]^\chi > 1 - \frac{1}{e^\chi}. \tag{3.5}$$

The number on the right is a limit of $P(m, n)$ for $m \to \infty$ and therefore a good lower estimate of this probability for $m$ finite. For instance for $m = 32$ the deviation is less than 1% and for bigger $m$ it is quickly decreasing.

## 3.2.2 Binomial Distribution

In the theory of probability and statistical modelling the binomial distribution plays an important role. It is a discrete probability distribution describing the probability of positive results in independent experiments.

More specifically, let us have a random quantity $X$ with two possible outcomes. The probability of the first (positive) outcome is $p$, the probability of the second (negative) outcome is $q = 1 - p$. We perform a sequence of $n$ independent experiments and ask what is the probability that we obtain the positive outcome exactly $k$ times. Of course $k$ can acquire only values $0, \ldots, n$.

The random quantity $X$ is characterized by the binomial distribution, which is described by the formula (see [2], page 140)

$$P(X = k) = \binom{n}{k} p^k q^{n-k}. \tag{3.6}$$

Similarly to other random distributions, the principal quantities characterizing the binomial distribution are the expected value $EX$ and the variance $DX$ (for

details see [2]). The value $EX$ can be obtained directly from the defining formula (3.6) by

$$EX = \sum_{k=0}^{n} k \binom{n}{k} p^k q^{n-k}.$$

The variance is defined by the relation

$$DX = E(X - EX)^2 = EX^2 - (EX)^2.$$

Several straightforward algebraic manipulations give us

$$EX = np$$

for the expected value and

$$DX = npq = np(1 - p)$$

for the variance.

### 3.2.3 Hypotheses Testing

In this part we briefly describe how to test the value of the parameter $p$ used in the definition of the binomial distribution on the basis of performed experiments.

Let us say we have an experiment with a positive and negative outcome described by the binomial distribution (3.6). We suppose that the probability of the positive outcome is $p_{\mathrm{pos}} = p_0$. This probability value represents the so called null hypothesis $H_0$

$$H_0 : p_{\mathrm{pos}} = p_0.$$

The validity of the hypothesis $H_0$ can be tested experimentally by performing the experiment $n$ times. Thus, we perform this experiment $n$ times and no positive result occurs. The question now is what conclusion can be made regarding the hypothesis $H_0$.

To quantify this situation we introduce a quantity called the significance level and denoted by $\alpha_{\mathrm{S}}$. The quantity $\alpha_{\mathrm{S}}$ represents the probability that we decline the hypothesis $H_0$ although it is true

$$\alpha_{\mathrm{S}} = P(H_0 \text{ true, but declined}),$$

where $P$ denotes the probability.

This indicates that we want to keep $\alpha_S$ reasonably small. Its value is usually put equal to alternatively $\alpha_S = 0.01$, $\alpha_S = 0.005$ or $\alpha_S = 0.001$. But it is just a common convention, its value can be chosen arbitrarily. In statistics, the quantity $\alpha_S$ is sometimes called the error of the first kind.

The hypotheses testing then works in the following way: We determine the critical part of the binomial distribution. In our circumstances it is the result

$$Bi(n, 0, p_0) = (1 - p_0)^n.$$

If $H_0$ is valid the probability of $Bi(n, 0, p_0)$ is small and decreasing with increasing $n$. The number of experiments $n$ has to be chosen, so that

$$Bi(n, 0, p_0) = (1 - p_0)^n < \alpha_S. \tag{3.7}$$

Since the result $Bi(n, 0, p_0)$ has a small probability, we interpret its occurrence as an indication that rather $H_0$ is false. This implies that the probability $p_{pos} < p_0$. This conclusion is not absolutely certain. There still exists a risk corresponding to the value $\alpha_S$ that $H_0$ is true implying $p_{pos} = p_0$.

Further, we can introduce a quantity $C_R$ called the relative certainty by the relation

$$C_R = 1 - \alpha_S.$$

Using the concept $C_R$ we can claim that $p_{pos} < p_0$ holds with the relative certainty $C_R$.

The situation can be also generalized to the case when some positive outcomes of the experiment occur. The difference is only in the fact how many positive outcomes we want to consider. This means that we extend the critical part of the distribution to the cases when we get positive outcomes. The probability of one positive outcome is according to (3.6)

$$Bi(n, 1, p_0) = \binom{n}{1} p_0 (1 - p_0)^{n-1} = \binom{n}{1} \frac{p_0}{1 - p_0} (1 - p_0)^n.$$

The probability of $k$ positive outcomes is

$$Bi(n, k, p_0) = \binom{n}{k} p_0^k (1 - p_0)^{k-1} = \binom{n}{k} \left( \frac{p_0}{1 - p_0} \right)^k (1 - p_0)^n.$$

When we declare that all the cases with $0, 1, \ldots, k$ positive outcomes belong to the critical part of the distribution we have to modify the relation (3.7) in the following way

$$\sum_{i=0}^{k} Bi(n, i, p_0) = (1 - p_0)^n \left[ 1 + \binom{n}{1} \frac{p_0}{1 - p_0}) + \cdots + \binom{n}{k} \left( \frac{p_0}{1 - p_0} \right)^k \right] < \alpha_{\mathrm{S}}.$$
(3.8)

From the relation (3.8) we can again determine the number of experiments $n$ necessary to perform to be able to decline the hypothesis $H_0$ with a reasonable risk of error less than $\alpha_{\mathrm{S}}$. We can formulate the following proposition.

**Proposition 3.2.1.** *Let us suppose we perform n experiments where n is determined by relation (3.8). If we obtain up to k positive outcomes, we can decline the hypothesis $H_0 : p_{\mathrm{pos}} = p_0$ with a risk at most $\alpha_{\mathrm{S}}$. In other words, we can claim that $p_{\mathrm{pos}} < p_0$ with the relative certainty $C_{\mathrm{R}} = 1 - \alpha_{\mathrm{S}}$.*

**Proof:** The proposition follows from the considerations that precede it.

### 3.2.4   An Example – Coin Flipping

Let us assume we have a regular coin with heads and tails sides. We expect that the probability to get the heads side should be equal to $\frac{1}{2}$. So, we form a null hypothesis $H_0$ claiming that the probability to get the heads $p_{\mathrm{h}}$ is equal to $p_0 = \frac{1}{2}$,

$$H_0 : p_{\mathrm{h}} = p_0 = \frac{1}{2}.$$

Now, we toss the coin several times and record the results. If the coin is really regular, we should get heads approximately in one half of experiments. If we get tails more often we can have a suspicion that the coin is not regular.

If we toss the coin several times and get no heads, we would like to make a conclusion regarding the value $p_{\mathrm{h}}$. The conclusion would probably be that the hypothesis $H_0$ is not valid that is that $p_{\mathrm{h}} < \frac{1}{2}$. But in principle we can also get the no heads result by a pure coincidence. The probability of this outcome on the assumption that $H_0$ is true is $(\frac{1}{2})^n$ when the coin was flipped $n$ times. So, the probability of such coincidence can be small, but such event is perfectly possible.

The only thing we can do is to flip the coin in some more experiments. Further no heads results support the conclusion that $H_0$ is not true indicating that $p_{\mathrm{h}} < \frac{1}{2}$.

In accordance with the previous part we choose significance levels $\alpha_{S1} = 0.01$, $\alpha_{S2} = 0.005$ and $\alpha_{S3} = 0.001$. If $H_0$ is true then the probability of no heads result in $n$ experiments amounts to

$$\left(1 - \frac{1}{2}\right)^n = \left(\frac{1}{2}\right)^n < \alpha_{S}.$$

Since these results are rather improbable for higher $n$, we say that their occurrence is caused rather by non validity of the hypothesis $H_0$. The term on the left side of the relation is smaller than $\alpha_{S1} = 0.01$ for $n_1 = 7$, for $\alpha_{S2} = 0.005$ for $n_2 = 8$ and for $\alpha_{S3} = 0.001$ for $n_3 = 10$.

The conclusion is that when we have the no heads result in 7 consecutive experiments we can claim with the relative certainty $C_{R1} = 0.99$ that the hypothesis $H_0$ is not valid which means $p_h < \frac{1}{2}$. When we have 8 consecutive experiments with no heads we can state the non validity of $H_0$ with the relative certainty $C_{R2} = 0.995$. With 10 consecutive no heads result we can claim that $H_0$ is not valid with the relative certainty $C_{R3} = 0.999$.

When we permit some positive results we have to use relation (3.8) instead of (3.7) for some specific value of $k$. As an example we present the cases when we get heads just once ($k = 1$) and twice ($k = 2$).
For $k = 1$ we get $n = 11$ to guarantee $C_R \geq 0.99$, $n = 12$ to guarantee $C_R \geq 0.995$ and $n = 14$ to guarantee $C_R \geq 0.999$. For $k = 2$ we get $n = 14$ to secure $C_R \geq 0.99$, $n = 15$ to secure $C_R \geq 0.995$ and $n = 18$ to secure $C_R \geq 0.999$.

## 3.3 Volume and Surface of a Ball in the $d$-dimensional Euclidean Space

In this section we present simple formulas for volumes and surfaces of a ball in the $d$-dimensional Euclidean space. These formulas are necessary for the subsequent probability estimates.

Volume and surface of a ball is usually expressed by means of the $\Gamma$ function in the form (see for instance book [38], page 316)

$$V_d(R) = \frac{\pi^{\frac{d}{2}}}{\Gamma(\frac{d}{2} + 1)} \cdot R^d \tag{3.9}$$

and

$$S_d(R) = \frac{2 \cdot \pi^{\frac{d}{2}}}{\Gamma(\frac{d}{2})} \cdot R^{d-1}. \tag{3.10}$$

Here $V_d(R)$ and $S_d(R)$ stand for the volume and surface of a ball with the radius $R$ in the $d$-dimensional Euclidean space. The $\Gamma$ function itself is defined by the integral formula

$$\Gamma(x) = \int_0^\infty e^{-t} t^{x-1} \, dx = 2 \int_0^\infty e^{-t^2} t^{2x-1} \, dx.$$

The integral is convergent for any real $x > 0$ and divergent for $x = 0$.

Nevertheless, after substituting for the term containing the $\Gamma$ function into the denominator we get different formulas for volumes and surfaces for even and odd dimensions:

$$V_{2k}(R) = \frac{\pi^k}{k!} \cdot R^{2k} \tag{3.11}$$

and

$$V_{2k+1}(R) = \frac{2^{k+1} \cdot \pi^k}{(2k+1)!!} \cdot R^{2k+1}, \quad k = 0, 1, 2, \ldots \tag{3.12}$$

for volumes and

$$S_{2k}(R) = \frac{2\pi^k}{(k-1)!} \cdot R^{2k-1} \tag{3.13}$$

and

$$S_{2k+1}(R) = \frac{2^{k+1} \cdot \pi^k}{(2k-1)!!} \cdot R^{2k}, \quad k = 1, 2, 3, \ldots \tag{3.14}$$

for surfaces. Here $k = 1, 2, \ldots$ In particular, the expressions for $d$ odd are rather clumsy.

By the term $n!!$ we denote here the double factorial of the integer $n$. The double factorial is defined as

$$n!! = n \cdot (n-2) \ldots 4 \cdot 2,$$

for $n$ even and

$$n!! = n \cdot (n-2) \ldots 3 \cdot 1,$$

for $n$ odd. We also define $1!! = 0!! = 1$.

All the expressions (3.11) – (3.14) have two principal disadvantages: They either contain $\Gamma$ function values that are not quite common to remember or lead to different formulas for even and odd dimensions. Therefore, we present equivalent simple formulas containing only elementary functions.

After some simple deductions and manipulations we get for the volume and surface of an $d$-dimensional ball with radius $R$ the following lemma.

**Lemma 3.3.1.** *The volume and surface of a ball of radius $R$ in the Euclidean space of dimension $d$ are given by the formulas*

$$V_d(R) = \frac{2^{\left\lceil \frac{d}{2} \right\rceil} \cdot \pi^{\left\lfloor \frac{d}{2} \right\rfloor}}{d!!} \cdot R^d, \quad d = 1, 2, 3, \ldots \tag{3.15}$$

*and*

$$S_d(R) = \frac{2^{\left\lceil \frac{d}{2} \right\rceil} \cdot \pi^{\left\lfloor \frac{d}{2} \right\rfloor}}{d!!} \cdot dR^{d-1}, \quad d = 1, 2, 3, \ldots \tag{3.16}$$

Here, the symbols $\lceil x \rceil$, $\lfloor x \rfloor$ stand for the upper and lower integer part of a number $x$, respectively.

**Proof:** In the current proof we demonstrate that the new formulas (3.15) and (3.16) are equivalent to formulas (3.9) and (3.10). The readers interested in the derivation of formulas (3.9) and (3.10) can consult the book [38] where the procedure of getting these relations is presented in full detail.

We suppose that the surface of the unit ball is in accordance with (3.10) given by the formula

$$S_d = \frac{2 \cdot \pi^{\frac{d}{2}}}{\Gamma(\frac{d}{2})}.$$

This implies $S_1 = 2$, $S_2 = 2\pi$.

Now, we take the ratio $\frac{S_d}{S_{d+2}}$. After some simple manipulations we get

$$\frac{S_d}{S_{d+2}} = \frac{d}{2\pi}.$$

Let us concentrate on the presented new formula (3.16) for the surface of the unit ball. We denote for a while the surface by $S'$ to be able to differentiate between original and new formulas.

$$S'_d = \frac{2^{\lceil \frac{d}{2} \rceil} \cdot \pi^{\lfloor \frac{d}{2} \rfloor}}{d!!} \cdot d.$$

We again form the first two terms, specifically $S'_1 = 2$ and $S'_2 = 2\pi$ which exactly corresponds to the previous results for the original formula. Analogously, we again take the ratio $\frac{S'_d}{S'_{d+2}}$. We also get

$$\frac{S'_d}{S'_{d+2}} = \frac{d}{2\pi}.$$

These ascertainments prove that both formulas for the surface of the unit ball are fully equivalent.

The surface of a ball with radius $R$ in the d-dimensional Euclidean space is then given by the formula

$$S_d = \frac{2^{\lceil \frac{d}{2} \rceil} \cdot \pi^{\lfloor \frac{d}{2} \rfloor}}{d!!} \cdot dR^{d-1}.$$

Since the volume and surface of a ball with radius $R$ are bound by the relations

$$S_d(R) = \frac{\mathrm{d}}{\mathrm{d}R} [V_d(R)]$$

and

$$V_d(R) = \int_0^R S_d(r)\mathrm{d}r,$$

it follows immediately that the volume of an d-dimensional ball is given by the formula

$$V_d(R) = \frac{2^{\left\lceil \frac{d}{2} \right\rceil} \cdot \pi^{\left\lfloor \frac{d}{2} \right\rfloor}}{d!!} \cdot R^d.$$

□

The deduced formulas (3.15) and (3.16) are not only simpler to use and easier to remember but also provide a certain insight how the formulas evolve with the increasing dimension $d$. The volumes and surfaces of balls in Euclidean spaces for several dimensions $d$ are presented in the Table 3.1.

| Dimension of the Euclidean space $d$ | Volume of a ball with radius $R$ $V_d(R)$ | Surface of a ball with radius $R$ $S_d(R)$ |
|---|---|---|
| 1 | $2R$ | $2$ |
| 2 | $\pi R^2$ | $2\pi R$ |
| 3 | $\frac{4}{3}\pi R^3$ | $4\pi R^2$ |
| 4 | $\frac{1}{2}\pi^2 R^4$ | $2\pi^2 R^3$ |
| 5 | $\frac{8}{15}\pi^2 R^5$ | $\frac{8}{3}\pi^2 R^4$ |
| 6 | $\frac{1}{6}\pi^3 R^6$ | $\pi^3 R^5$ |
| 7 | $\frac{16}{105}\pi^3 R^7$ | $\frac{16}{15}\pi^3 R^6$ |
| 8 | $\frac{1}{24}\pi^4 R^8$ | $\frac{1}{3}\pi^4 R^7$ |
| 9 | $\frac{32}{945}\pi^4 R^9$ | $\frac{32}{105}\pi^4 R^8$ |
| 10 | $\frac{1}{120}\pi^5 R^{10}$ | $\frac{1}{12}\pi^5 R^9$ |
| 12 | $\frac{1}{720}\pi^6 R^{12}$ | $\frac{1}{60}\pi^6 R^{11}$ |
| 14 | $\frac{1}{5040}\pi^7 R^{14}$ | $\frac{1}{360}\pi^7 R^{13}$ |
| 16 | $\frac{1}{40320}\pi^8 R^{16}$ | $\frac{1}{2520}\pi^8 R^{15}$ |

Table 3.1: Dependence of the volume and surface of a ball on the dimension of the Euclidean space into which the ball is embedded

From the Table 3.1 it is obvious that the volume $V_d(R)$ of a ball with fixed radius $R$ quickly decreases with the increasing dimension $d$ of the Euclidean

space into which the ball is embedded. More specifically, for a fixed radius $R$ the volume $V_d(R)$ approaches 0 when $d$ tends to $\infty$. The following lemma describes the asymptotic behaviour of $V_d(R)$ for $d \to \infty$.

**Corollary 3.3.2.** *The volume $V_d(R)$ of a ball with radius $R$ in the d-dimensional Euclidean space for $d \to \infty$ can be estimated by the formula*

$$V_d(R) \sim \frac{1}{\sqrt{\pi d}} \left( \frac{2\pi e}{d} \right)^{\frac{d}{2}} R^d. \tag{3.17}$$

**Proof:** Let us take the formula (3.15) for the volume of a ball with radius $R$ in the $d$-dimensional Euclidean space, $d$ even ($d = 2k$, k $= 0, 1, 2, \dots$). Then we have

$$V_d(R) = \frac{2^{\frac{d}{2}} \cdot \pi^{\frac{d}{2}}}{d!!} \cdot R^d, \quad d = 0, 1, 2, \dots \tag{3.18}$$

For $n = 2k$ the following relation for double factorials holds

$$n!! = 2^k k!.$$

The double factorial in the denominator of (3.18) can then be expressed as

$$d!! = 2^{\frac{d}{2}} \left( \frac{d}{2} \right)!.$$

This means we have

$$V_d(R) = \frac{\pi^{\frac{d}{2}}}{\left( \frac{d}{2} \right)!} \cdot R^d, \quad d = 0, 1, 2, \dots$$

Now, we apply the Stirling formula for the term containing the factorial

$$n! \sim \sqrt{2\pi n} \left( \frac{n}{e} \right)^n, \quad n \to \infty,$$

implying

$$\left( \frac{d}{2} \right)! \sim \sqrt{\pi d} \left( \frac{d}{2e} \right)^{\frac{d}{2}}, \quad d \to \infty.$$

This finally provides

$$V_d(R) \sim \frac{1}{\sqrt{\pi d}} \left( \frac{2\pi e}{d} \right)^{\frac{d}{2}} \cdot R^d, \quad d \to \infty.$$

$\square$

**Remark 3.3.1.** *Since the Stirling approximation is a lower estimate of the corresponding factorial value, the formula (3.17) is in fact an upper bound for the volume of a d-dimensional ball.*

# Chapter 4

# Radiation Heating Model

We need a suitable mathematical model to analyze the radiation heating of the shell mould. We model the infrared heaters and the mould in a three dimensional Euclidean space $\mathbb{R}^3$ with Cartesian coordinate system $(O, x_1, x_2, x_3)$ and the base vectors $e_1 = (1, 0, 0)$, $e_2 = (0, 1, 0)$ and $e_3 = (0, 0, 1)$.

## 4.1  Heater Representation

Each heater is represented by a straight line segment with length $d$ (see the left part of Figure 4.1). The position of the heater is described by the following parameters:

(i) The coordinates of the centre of the heater $C = [C_1, C_2, C_3]$.

(ii) The unit vector $u = (u_1, u_2, u_3)$ that is oriented in the direction of the maximal heat radiation. We shall suppose that the component $u_3 < 0$ which means that the heater radiates downward.

(iii) The unit vector $r = (r_1, r_2, r_3)$ in the direction of the longitudinal heater axis $o$.

In this case we would have 9 quantities describing the position and orientation of the heater. Nevertheless, some of these quantities are dependent. For instance the vectors $u$ and $r$ are perpendicular.

It is a well known fact in mechanics of a solid body that for the full description of the position and orientation of the body in the three dimensional space 6 parameters are sufficient. That means that it is necessary to reduce the number
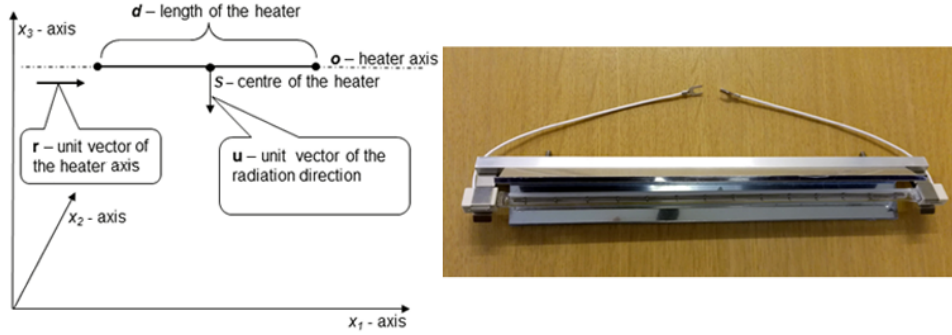
Figure 4.1: The model of the infrared heater (left) and an example of a real heater (right)

of quantities that determine the position of the heater. It is convenient to use the first two coordinates $u_1$, $u_2$ of the vector $u$. The vector $r$ can then be described by one parameter, for instance by angle $\phi$ between its vertical projection onto the horizontal plane $x_1 x_2$ and the positive part of the axis $x_1$ ($0 \leq \phi < \pi$). Thus the position of each heater $H_i$, $i = 1, \ldots, M$, can be fully and uniquely defined by the following 6 parameters

$$H_i = (C_1^i, C_2^i, C_3^i, u_1^i, u_2^i, \phi^i). \tag{4.1}$$

## 4.2 Heat Flux Modelling

In this part we give a brief account how we evaluate the radiation heat flux coming onto the mould surface. In principle, we have to combine several entities. First, we need an adequate approximate model of the mould surface. Second, it is necessary to know how the generated heat radiation intensity is distributed in the neighbourhood of the heater. Third, we also need a reasonable prescription how to combine the radiation intensity incident onto the mould surface simultaneously from several heaters. We start with a suitable approximate model of the mould.

### 4.2.1 Mould Representation

The outer mould surface $P$ can be described by small elementary surfaces $p_j$, where $1 \leq j \leq N$, such that

$$P = \bigcup_{j=1}^{N} p_j \quad \text{and} \quad (\text{int } p_i) \cap (\text{int } p_j) = \emptyset \quad \text{for} \quad i \neq j, 1 \leq i \leq N, 1 \leq j \leq N,$$

where $\text{int } p_i$ denotes the interior of elementary surface $p_i$.

Each elementary surface $p_j$ can be determined by the following parameters:

(i) The centroid $T_j = [T_1^j, T_2^j, T_3^j]$ of the elementary surface $p_j$.

(ii) The unit vector of the outer normal $v_j = (v_1^j, v_2^j, v_3^j)$ at the point $T_j$ (we can suppose $v_j$ faces "upwards" and therefore is defined through the first two components $v_1^j$ and $v_2^j$).

(iii) The area $c_j$ of the elementary surface.

Each elementary surface $p_j$ can then be defined by the following 6 parameters

$$p_j = (T_1^j, T_2^j, T_3^j, v_1^j, v_2^j, c_j). \tag{4.2}$$

## 4.2.2   Calculation of the Heat Radiation Intensity on an Elementary Surface

To be able to calculate the heat radiation intensity incident on each elementary surface from one heater we need to know how the heat radiation intensity is distributed in space in the heater neighbourhood. The heaters manufacturers do not usually provide such heat radiation distribution diagrams which describe the heat radiation intensity field around the heater. These heating diagrams for individual types of heaters have to be determined experimentally.

The measuring of these heat radiation diagrams does not form a part of this thesis. The detailed description of the experimental arrangement can be found in article [23].

## 4.2.3   Heat Radiation Intensity and Uniformity of Its Distribution

Now, we describe the numerical computation of the heat radiation intensity on the mould surface. Let us suppose that all the heaters are located in fixed positions. We denote by $L_j$ the set of all heaters radiating on the $j$-th elementary surface $p_j$

$(1 \leq j \leq N)$. By $I_{jl}$ we denote the heat radiation intensity from the $l$-th heater incident on the $p_j$ elementary surface. Then the total radiation intensity $I_j$ on the elementary surface $p_j$ is according to [5] given by

$$I_j = \sum_{l \in L_j} I_{jl} \; . \tag{4.3}$$

The producer of artificial leather recommends a constant value of the heat radiation intensity on the heated surface of the mould. Let us denote this constant value as $I_{\mathrm{rec}}$. This specific value is hardly attainable with a limited number of heaters. The goal is to achieve approximately uniform intensity close to the recommended value on the whole heated mould surface. We can define a deviation function $F(H_1, H_2, \ldots, H_M)$ that quantifies the deviation of the intensity from the recommended value $I_{\mathrm{rec}}$ by

$$F = \frac{1}{W} \sum_{j=1}^{N} (I_j - I_{\mathrm{rec}})^2 \, c_j \; , \tag{4.4}$$

where $W = \sum_{j=1}^{N} c_j$. Let us recall that $c_j$ denotes the area of elementary surface $p_j$. Each symbol $H_i$ represents six parameters describing the position and orientation of an individual heater.

Thus, the arguments of the deviation functions are $6 \cdot M$ parameters describing the positions and orientations of all heaters in compliance with (4.1). We need to find such locations of the heaters that minimize the value of deviation function $F(H_1, H_2, \ldots, H_M)$.

# Chapter 5

# Optimization of the Heat Flux Distribution

In this chapter we present techniques used to optimize the heat flux distribution on the heated side of the mould. The optimization is realized by means of differential evolution algorithms. It is shown that the original differential evolution algorithm does not guarantee the global convergence. Therefore, the original differential evolution algorithm was modified with the aim to increase the potential to identify the global minimum of the cost function. The chapter also includes some theoretical and practical conclusions regarding the original and modified algorithm.

## 5.1 General Remarks and Concepts Introduction

In general, optimization tasks represent an important part of application mathematics. The optimization algorithms are frequently used in engineering, science and production practice. Besides, optimization is a fascinating area of study because of its universal applicability. Broadly speaking, to optimize a system means to maximize the system's desirable properties minimizing simultaneously its unfavourable characteristics.

The optimized system has several parameters that influence the property being optimized. The optimization task can typically be described by means of an objective function. The parameters of the system then represent the variables of

the objective function. The optimization problem is then transformed into the task to identify extreme values of this objective function. When we search for the minimum of the objective function then the term cost function is mostly used. On the other hand if we look for the maximum of the objective function then the term fitness function is usual. For an extensive survey of various optimization techniques see for instance books [35] or [39].

## 5.2   Evolutionary Computing

At present, evolutionary algorithms (including differential evolution algorithms) are used for optimization tasks with intricate costs functions and complicated constraints. The evolutionary algorithms are primarily utilized in situations when other usual methods fail to converge to the optimized stated. For example the commonly used gradient methods require that the cost function is differentiable. Additionally, they mostly do not identify the global minimum when the cost function has a lot of local minima. In these cases the gradient methods are prone to converge to a local minimum. This means that their results strongly depend on the choice of the search starting point.

The evolutionary methods try to overcome this problem by a different approach. They create whole generations of potential solutions. The creation of potential solutions is partly random. This contributes to more extensive exploring of the cost function domain. The potential solutions are then assessed according to their cost function value. The solutions with lower cost function values have better prospects to take part in the creation of the subsequent generation.

Evolutionary algorithms are formed in principal by two main groups. The first group is the family of genetic algorithms. The algorithms in this group simulate quite closely the natural selection in nature. For instance they utilize a cross over and mutation mechanisms when creating new individuals (potential solutions). The genetic algorithms are extensively studied in the book [1] and [21]. The second group consists of differential evolution algorithms. In this work we focus primarily on differential evolutions algorithms.

These algorithms were first introduced by Storn and Price in [34] and [41]. Because of the random creation of individual potential solutions, the convergence analysis of differential algorithms is relatively demanding. This is probably the reason why the published results concerning the sufficient conditions for the global

convergence of the differential evolution algorithms are relatively rare.

The differential evolution algorithms now consist of a larger group of similar algorithms that differ in implementation details. We concentrate on the standard $DE/rand/1/bin$ algorithm which is best known and mostly used. That is why it is termed as the classic differential evolution algorithm in [35]. Hereafter it is referenced to as CDEA.

## 5.3   Classic Differential Evolution Algorithm

In this part we briefly describe the operation of CDEA. Generally, CDEA seeks for the minimum of the cost function by constructing whole generations of individuals. Each individual is an ordered set of specific values corresponding to one point from the cost function domain. In this way each individual represents a potential solution of the optimization task. The quality of this individual is determined by the evaluation of the cost function corresponding to this individual.

The next generation is formed from the existing generation by means of mutation and crossover operators. Specifically, we go successively through all individuals in the generation $G$. To each individual $y_i^G$ (termed as the *target individual*) we select randomly three other (different) individuals $y_{r1}^G, y_{r2}^G, y_{r3}^G$ from the current generation. We form in a specific way (including randomness) a combination of these three individuals and the target individual. This combination is termed as the *trial individual* and denoted $y_i^{\text{trial}}$. Then we evaluate the cost function for the target $y_i^G$ and trial individual $y_i^{\text{trial}}$ and compare the results. The individual with lower value of the cost function advances to the position of the target individual of the next generation $y_i^{G+1}$. When this procedure is completed for all target individuals in generation $G$, we have the new generation of individuals numbered $G + 1$.

The next part illustrates CDEA operation more specifically in the form of the pseudo code.

**Input:**
Optimization task parameters:
$f$ denotes the cost function, $D$ is the dimension of the cost function domain, $\langle x_{i\text{min}}, x_{i\text{max}} \rangle$ is a domain of each cost function variable $x_i$.
CDEA parameters:

$NP$ denotes the generation size (the number of individuals in each generation), $NG$ is the total number of generations, $F$ stands for the mutation factor, $F \in \langle 0, 2 \rangle$, and $CR$ denotes the crossover probability, $CR \in \langle 0, 1 \rangle$. The symbol $G$ stands for the generation number, index $i$ is the number of the individual in the generation, index $j$ describes the $j$-th component of a specific individual $y_i$.

**Computation:**

1. create the initial generation ($G = 1$) of $NP$ individuals $y_i^G$, $1 \le i \le NP$, randomly or according to a prescribed scheme

2. (a) evaluate all individuals $y_i^G$ of the generation $G$ (calculate $f(y_i^G)$ for each individual $y_i^G$)

   (b) store the individuals $y_i^G$ and their evaluations $f(y_i^G)$ into the matrix $\mathbf{A}$ with $NP$ rows and $D + 1$ columns

3. ***repeat until*** $G \le NG$

   (a) ***for*** $i = 1$ ***to*** $NP$ ***do***

      i. randomly select three different indices $r_1, r_2, r_3 \in \{1, 2, \ldots, NP\}$, $r_m \ne i,\ m \in \{1, 2, 3\}$

      ii. randomly select an index $k_i \in \{1, \ldots, D\}$

      iii. ***for*** $j = 1$ ***to*** $D$ ***do***

      $\quad$ ***if*** $(rand\langle 0, 1 \rangle \le CR$ ***or*** $j = k_i)$
      $\quad\quad$ ***then*** $y_{i,j}^{\text{trial}} = y_{r3,j}^G + F(y_{r1,j}^G - y_{r2,j}^G)$
      $\quad\quad$ ***else*** $y_{i,j}^{\text{trial}} = y_{i,j}^G$
      $\quad$ ***endif***

      $\quad$ ***endfor(j)***

      iv. ***if*** $f(y_i^{\text{trial}}) \le f(y_i^G)$
      $\quad\quad$ ***then*** $y_i^{G+1} = y_i^{\text{trial}}$
      $\quad\quad$ ***else*** $y_i^{G+1} = y_i^G$
      $\quad$ ***endif***

      ***endfor(i)***

   (b) store the individuals $y_i^{G+1}$ and their evaluations $f(y_i^{G+1}), 1 \le i \le NP$, of the new generation $G + 1$ into the matrix $\mathbf{A}$, $G = G + 1$

   ***endrepeat.***

**Output:**

The matrix $\mathbf{A}$ with $NP$ rows and $D+1$ columns contains the final generation of individuals including their evaluations. The row of matrix $\mathbf{A}$ that contains the lowest cost function value represents the best found individual $y_{\min}$.

# 5.4 Classic Differential Evolution Algorithm and the Global Convergence

In this part we present some simple considerations indicating that the CDEA has in some simple situations rather limited ability to determine the global minimum of the cost function. The conclusion following from this fact is that the CDEA guarantees in general only the convergence to a local minimum of the cost function. We demonstrate this fact by means of a specific cost function.

## 5.4.1 Counterexample to Global Convergence of CDEA

It is not difficult to find counterexamples to the global convergence of the CDEA. Let us consider for instance the following two graphs of cost functions with the domain in Euclidean space $\mathbb{R}^2$, see Figure 5.1.

Even for the cost function shown in Figure 5.1(a) the probability that the CDEA finds the global minimum of the cost function is less than one. The reason is that the CDEA can converge in some cases relatively fast to the local minimum missing completely the global minimum. This results in concentrating the individuals in subsequent generations around the local minimum. As soon as the size of the generation falls under some critical value, the generation is too small to produce trial individuals that could hit the the region around the global minimum. This situation is called *a premature convergence*. In this case even increasing the number of generations does not lead to increasing the chances to find the global minimum.

Moreover, the probability that the CDEA finds the global minimum falls with the decreasing measure of the global minimum region. The probability of finding the global minimum for the cost function in Figure 5.1(b) is substantially smaller than for the cost function in Figure 5.1(a). Additionally, by a sufficient reduction of the measure of the global minimum region this probability can be made as close to zero as possible.
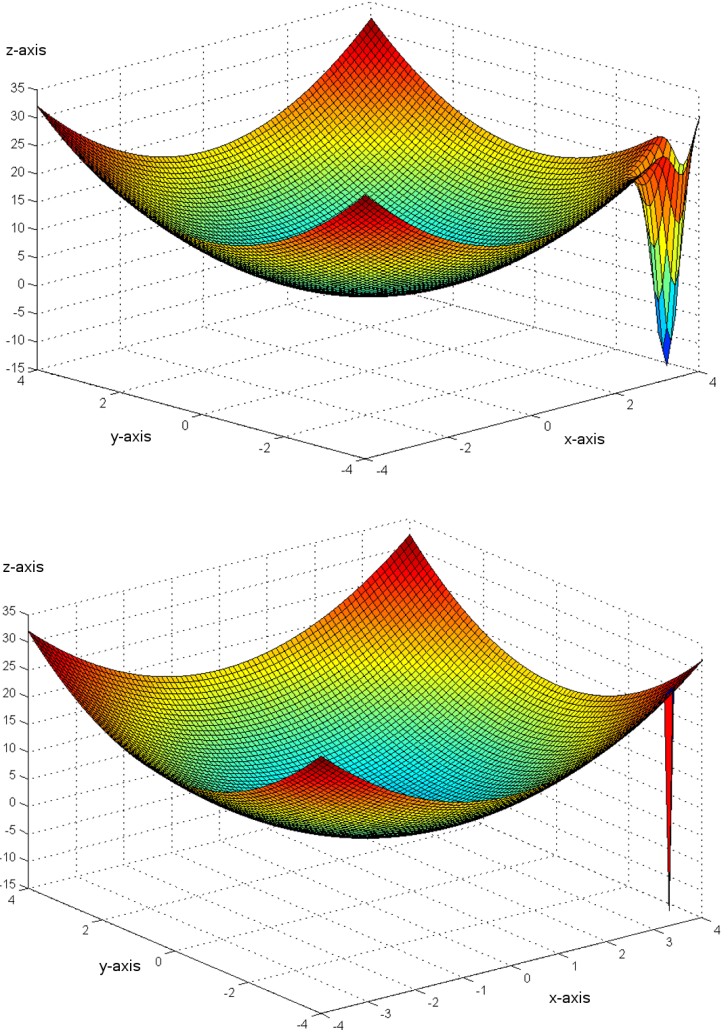
Figure 5.1: Examples of cost functions with domains in $\mathbb{R}^2$

## 5.4.2   Numerical Example Description

We can present a specific cost function to demonstrate the limited ability of CDEA to converge to the global minimum of the cost function. To keep things simple we consider the domain of the cost function as a subset of the two-dimensional Euclidean space $\mathbb{R}^2$. We will construct the cost function $F(x_1, x_2)$ as a composition of two simple functions

$$F(x_1, x_2) = F_\mathrm{B}(x_1, x_2) + F_\mathrm{M}(x_1, x_2). \tag{5.1}$$

The term $F_\mathrm{B}(x_1, x_2)$ represents the base function. This function should be smooth, relatively shallow and attain one minimum. It can be defined for instance in the following way

$$F_\mathrm{B}(x_1, x_2) = x_1^2 + x_2^2,$$

with the domain $D(F_\mathrm{B}) = \langle -H, H \rangle \times \langle -H, H \rangle$, where $H$ determines the boundary values of the domain.

The term $F_\mathrm{M}(x_1, x_2)$ denotes a modifier function. This function should be relatively steep and with a rather small domain. We use the function $F_\mathrm{M}(x_1, x_2)$ to modify the underlying base function $F_\mathrm{B}(x_1, x_2)$. The role of the function $F_\mathrm{M}(x_1, x_2)$ is to realize the global minimum of the cost function $F(x_1, x_2)$. To be able to construct the function $F_\mathrm{M}(x_1, x_2)$ effectively, we introduce another auxiliary function $F_\mathrm{P}(x_1, x_2)$

$$F_\mathrm{P}(x_1, x_2) = x_1^2 + x_2^2 - 1,$$

with the domain $D(F_\mathrm{P}) = \{x_1, x_2 : x_1^2 + x_2^2 \leq 1\}$.

It is obvious that the function $F_\mathrm{P}(x_1, x_2)$ is defined exclusively on a unit circle and attains values from the closed interval $\langle -1, 0 \rangle$. The graph of the function $F_\mathrm{P}(x_1, x_2)$ is a circular paraboloid presented in Figure 5.2.

The function $F_\mathrm{M}(x_1, x_2)$ is then formed as

$$F_\mathrm{M}(x_1, x_2) = \lambda_\mathrm{h} \cdot F_\mathrm{P}\left(\frac{1}{\rho}(x_1 - x_\mathrm{G1}), \frac{1}{\rho}(x_2 - x_\mathrm{G2})\right).$$

Here the number $\lambda_\mathrm{h}$ defines the height of the resulting circular paraboloid, $\rho$ denotes the radius of the domain on which the modifier function $F_\mathrm{M}(x_1, x_2)$ is defined. Obviously, the modifier function $F_\mathrm{M}(x_1, x_2)$ is defined only for points that are closer to the point $[x_\mathrm{G1}, x_\mathrm{G2}]$ than the radius of its domain $\rho$. The
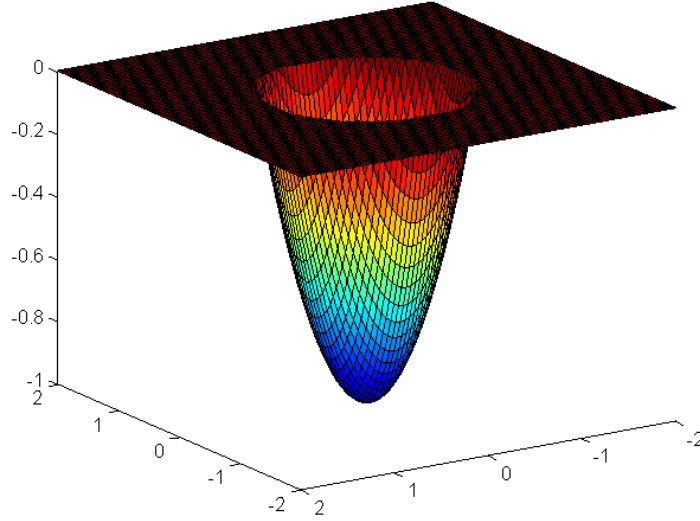
Figure 5.2: Graph of the auxiliary function $F_{\mathrm{P}}(x_1, x_2)$

coordinates $x_{\mathrm{G1}}$, $x_{\mathrm{G2}}$ specify the point, where the modifier function $F_{\mathrm{M}}(x_1, x_2)$ attains its minimum.

The overall cost function $F(x_1, x_2)$ is then defined according to the relation (5.1) by the composite formula

$$F(x_1, x_2) = x_1^2 + x_2^2 + \lambda_{\mathrm{h}} \cdot F_{\mathrm{P}} \left( \frac{1}{\rho}(x_1 - x_{\mathrm{G1}}), \frac{1}{\rho}(x_2 - x_{\mathrm{G2}}) \right). \qquad (5.2)$$

We have to choose the parameters $\lambda_{\mathrm{h}}$, $\rho$, $x_{\mathrm{G1}}$ and $x_{\mathrm{G2}}$ in a reasonable way to attain the required result. It is clear that we can control the dimensions of modifier function domain by the parameter $\rho$. The point $[x_{\mathrm{G1}}, x_{\mathrm{G2}}]$ is to be placed relatively close to the boundary of the cost function domain. This means it is relatively far from the point $[0, 0]$ representing the local minimum of the cost function analogously to the cost functions presented in Figure 5.1.

Since the base function $F_{\mathrm{B}}(x_1, x_2)$ is positive definite, it attains a positive value $F_{\mathrm{B}}(x_{\mathrm{G1}}, x_{\mathrm{G2}})$ at the point $[x_{\mathrm{G1}}, x_{\mathrm{G2}}]$. This means we have to take the parameter $\lambda_{\mathrm{h}}$ sufficiently large, so that the global minimum is essentially lower than the local minimum at the point $[0, 0]$. A reasonable value for $\lambda_{\mathrm{h}}$ is $2F_{\mathrm{B}}(x_{\mathrm{G1}}, x_{\mathrm{G2}})$. This choice implies that the cost function value $F(x_{\mathrm{G1}}, x_{\mathrm{G2}})$ at the point $[x_{\mathrm{G1}}, x_{\mathrm{G2}}]$ is $-F_{\mathrm{B}}(x_{\mathrm{G1}}, x_{\mathrm{G2}})$ and thus substantially lower than the value $F(0, 0) = 0$ at the point $[0, 0]$ representing the local minimum of the cost function $F(x_1, x_2)$.

This simple setting has one more important advantage. As mentioned before, the CDEA is greedy. This means it does not abandon a point with a low cost function value unless it finds a point with an even lower cost function value. This fact implies that to find the global minimum of the cost function $F(x_1, x_2)$ in our case, it is not enough to hit only the part of the cost function domain $F(x_1, x_2)$, where the modifier function $F_{\mathrm{M}}(x_1, x_2)$ is defined. It is necessary to hit a point from the modifier function $F_{\mathrm{M}}(x_1, x_2)$ domain, where the value of $F(x_1, x_2)$ is lower than at the local minimum at the point $[0, 0]$. If the algorithm hits such a point it never abandons it unless it goes further closer to the global minimum of the cost function $F(x_1, x_2)$. This indicates the subsequent convergence of the algorithm to the global minimum.

So, it is important to have the information what is the measure of $F_{\mathrm{M}}(x_1, x_2)$ domain with $F(x_1, x_2)$ values lower than the value at the local minimum. In our setting this measure can easily be calculated. In fact, it is exactly one half of the measure of $F_{\mathrm{M}}(x_1, x_2)$ domain. This fact makes possible to compare the results of CDEA statistical testing with our preliminary probability expectations.
Specific parameters of the cost function $F(x_1, x_2)$:
We put $H = 4$. This value indicates that the domain of the cost function $F(x_1, x_2)$ is a set $\langle -4, 4 \rangle \times \langle -4, 4 \rangle$ with the measure $\mu(D(F)) = 8^2 = 64$.
We set $x_{1\mathrm{G}} = x_{2\mathrm{G}} = 3$. This means that the global minimum of the cost function $F(x_1, x_2)$ is at the point $[3, 3]$ and the base function value at this point is $F_{\mathrm{B}}(3, 3) = 3^2 + 3^2 = 18$.
We put $\lambda_{\mathrm{h}} = 36$. This value implies the cost function value $F(3, 3)$ at the global minimum to be $-18$.
We set $\rho = \frac{1}{10}$. This determines the radius of the domain of the modifier function $F_{\mathrm{M}}(x_1, x_2)$. The measure of the modifier cost function domain is $\mu(D(F_{\mathrm{M}})) = \pi \rho^2 \doteq 3.14 \cdot (\frac{1}{10})^2 = 0.0314$.

From the above mentioned it follows that the measure of the part of the cost function domain $F(x_1, x_2)$ with values less than the value at the point of the local minimum is

$$\mu(D(F) \cap (F(x_1, x_2) \leq F(0, 0)) = \tfrac{1}{2}\pi\rho^2 \doteq 0.0157.$$

### 5.4.3 Numerical Example Statistics

The above mentioned numerical example was programmed in the Matlab environment to verify the hypothesis that the success rate of CDEA in finding the global

minimum of the cost function under such circumstances is relatively low. We performed 200 numerical experiments with the following parameters: number of individuals in each generation $NP = 200$, number of generation $NG = 160$. The algorithm CDEA identified the global minimum of the cost function $F(x_1, x_2)$ in 37 cases out of 200. In 163 experiments the CDEA ended up at the local minimum of $F(x_1, x_2)$ at the point $[0, 0]$. This gives a conclusion that CDEA finds under such circumstances the global minimum of the cost function only in approximately 18.5% of cases which is rather poor result.

Additionally, the success rate can be lowered arbitrarily by reducing the quantity $\rho$ implying the decrease in the measure of the region with the cost function values below the cost function value at the local minimum.

To demonstrate this fact, we reduced the parameter $\rho$ to $\frac{1}{16}$ and peformed another 200 experiments. This time the algorithm CDEA identified the global minimum of the cost function $F(x_1, x_2)$ in 15 cases out of 200. In 185 experiments the CDEA ended up at the local minimum of $F(x_1, x_2)$ at the point $[0, 0]$. This gives a percentage success rate to identify the global minimum only 7.5%.

These results illustrating the limited ability of CDEA to identify the global minimum under these circumstances are summarized in the following table.

| CDEA | Local minimum hits | Global minimum hits | Success rate in % |
|---|---|---|---|
| $\rho = \frac{1}{10}$ | 163 | 37 | 18.5 |
| $\rho = \frac{1}{16}$ | 185 | 15 | 7.5 |

Table 5.1: Experimental testing of CDEA

Another unfavourable feature of CDEA is the fact that even if the number of generations $NG$ is essentially increased it does not lead to a higher success rate, because if the algorithm does not hit the region of the global minimum in several first generations the subsequent generations concentrate relatively quickly around the local minimum. Losing generations diversity results in impossibility to hit the region of the global minimum in any of the following generations.

## 5.5 Modified Differential Evolution Algorithm

In the first part of this section we describe the modification of CDEA called MDEA ensuring the asymptotic global convergence. In the second part we present better global convergence abilities of MDEA by a numerical example including simple statistics.

### 5.5.1 Modification to Ensure the Asymptotic Global Convergence

As mentioned in the previous part, CDEA does not in general guarantee the convergence to the global minimum of the cost function. This is caused by the too fast convergence of CDEA to the local minimum (premature convergence) resulting in rapid reduction of the generation size (loss of diversity). This observation gives us a hint how to modify CDEA, so that it provides better results regarding the global convergence. The most straightforward way is to limit the premature convergence by replacing some individuals with the highest values of the cost function in each generation by random individuals. Though these random individuals reduce partially the convergence speed they increase substantially the diversity of the generation. The increased diversity ensures then even the asymptotic global convergence of the modified algorithm.

Therefore, it is in principle necessary to make one simple change in the algorithm. We present only the differences with respect to CDEA. See the pseudo-code description of CDEA in Chapter 5.3.

**Input:**

We add another parameter $R$ that determines the ratio of random individuals in each generation, $R \in \langle 0, 1 \rangle$, e.g., $R = 0.1$ means that 10% of individuals in each generation are generated randomly.

**Computation:**

We add another procedure to the part (3), specifically:

(c) determine in matrix $\mathbf{A}$ the quantity $\lfloor NP \cdot R \rfloor$ of individuals with the highest cost function values and replace these individuals by random individuals from the search space.

Here the symbol $\lfloor x \rfloor$ denotes the integer part of the real number $x$.

## 5.5.2   Numerical Example: Comparison CDEA - MDEA

We can perform the same testing using the identical cost function $F(x_1, x_2)$ defined by the relation (5.2) with MDEA. All parameters of the test are the same as before: number of individuals in each generation $NP = 200$, number of generations $NG = 160$, the number of experiments again 200. Additionally, for MDEA it is necessary to set the value $R$ specifying the ratio of random individuals in each generation. We put $R = 0.1$ implying 10 % of random individuals in each generation.

The algorithm MDEA identified the global minimum of the cost function $F(x_1, x_2)$ in 166 cases out of 200 for $\rho = \frac{1}{10}$ and in 130 cases out of 200 for $\rho = \frac{1}{16}$. The results are summarized in the Table 5.2.

| CDEA | | | MDEA | | |
|---|---|---|---|---|---|
| Local minimum hits | Global minimum hits | Success rate in % | Local minimum hits | Global minimum hits | Success rate in % |
| 163 | 37 | 18.5 | 34 | 166 | 83.0 |
| 185 | 15 | 7.5 | 70 | 130 | 65.0 |

Table 5.2: Experimental comparison of CDEA and MDEA. The first row represents the data for $\rho = \frac{1}{10}$, the second row presents the data for $\rho = \frac{1}{16}$.

Another positive feature of the algorithm MDEA is that if we increase the number of generations $NG$ the global minimum will be identified with an increased probability. This probability can come close to 1 for a sufficiently high number of generations. We call this aspect of the MDEA an asymptotic global convergence. We describe this topic in the following part.

## 5.6    Asymptotic Global Convergence

In this part we present several theoretical concepts and statements that can be used to prove the asymptotic global convergence of MDEA. More specifically, we are able to show that when the number of generations $G \to \infty$ than the probability that MDEA finds the global minimum of the cost function approaches 1.

### 5.6.1    Optimal Solution Set

We have an optimization task to identify the minimum of a cost function $F(x_1, x_2, \ldots, x_d)$ defined on an $d$-dimensional bounded domain. For brevity we denote by the symbol $x$ the ordered $d$-tuple $x_1, x_2, \ldots, x_d$. In this notation $x = (x_1, x_2, \ldots, x_d)$. That is we should find the minimum of the function $F(x)$. In general this function may have more local and global minima. We would like to find the minimum with the lowest cost function value

$$\min\{F(x) : x \in S\}, \tag{5.3}$$

where $S$ is a measurable search space of a finite measure representing all possible configurations of variables $x$. We suppose that the global minimum of function $F$ exists on $S$. The solution set can be defined as

$$S^* = \{x^* : F(x^*) = \min\{F(x) : x \in S\}\},$$

where $x^*$ represent global minima of the function $F$. To be able to prove the convergence in probability we consider an expanded solution set

$$S_\varepsilon^* = \{x \in S : |F(x) - F(x^*)| < \varepsilon\}, \tag{5.4}$$

where $\varepsilon > 0$ is a small positive real number. Denoting by $\mu$ the Lebesgue measure, we suppose that for each $\varepsilon$ it holds that $\mu(S_\varepsilon^*) > 0$.

**Definition 5.6.1.** *We call the set $S_\varepsilon^*$ defined by relation (5.4) the optimal solution set.*

### 5.6.2    Convergence in Probability

To examine the global convergence of MDEA we need to introduce a concept of the convergence in probability defined in [11].

**Definition 5.6.2.** *Let $\{G(k), k = 1, 2, \ldots\}$ be a generation sequence created by a differential evolution algorithm to solve the optimization problem (5.3). We say that the algorithm converges to the optimal solution set in probability if*

$$\lim_{k \to \infty} p\{G(k) \cap S_\varepsilon^* \neq \emptyset\} = 1, \tag{5.5}$$

*where $p$ denotes the probability of an event.*

Now we can prove the following theorem.

**Theorem 5.6.1.** *Let us suppose that for each generation $G(k)$ of a differential evolution algorithm there exists at least one individual $y$ such that*

$$p\{y \in S_\varepsilon^*\} \geq \alpha > 0,$$

*where $\alpha$ is a small positive value. Then the algorithm converges to the optimal solution set $S_\varepsilon^*$ in probability. That is the relation (5.5) holds.*

Here $p\{y \in S_\varepsilon^*\}$ denotes the probability that $y$ belongs to the optimal solution set $S_\varepsilon^*$.

**Proof:** Let us suppose that an individual $y^{\text{rand}} \in S$ is created randomly in each generation $G(k)$. The probability that it hits the optimal solution set is given by the relation

$$p\{y^{\text{rand}} \in S_\varepsilon^*\} = \frac{\mu(S_\varepsilon^*)}{\mu(S)} = \alpha > 0.$$

It means that the relation

$$p\{y^{\text{rand}} \notin S_\varepsilon^*\} = 1 - \alpha$$

holds for each generation. We can estimate that the first $k$ generations do not include an individual $y \in S_\varepsilon^*$ by the relation

$$\prod_{i=1}^{k} p\{G(i) \cap S_\varepsilon^* = \emptyset\} \leq (1 - \alpha)^k.$$

The inequality in this relation follows from the fact that in principle the set $S_\varepsilon^*$ can be achieved not only by random individuals but also by the individuals that were created by the differential evolution mechanism. Based on the construction of individuals in generation $G(k)$, the best individual in generation $G(k)$ has

the same or better evaluation than the best individual from all the previous generations implying

$$\lim_{k\to\infty} p\{G(k) \cap S_\varepsilon^* = \emptyset\} = \lim_{k\to\infty} \prod_{i=1}^{k} p\{G(i) \cap S_\varepsilon^* = \emptyset\} \leq \lim_{k\to\infty} (1-\alpha)^k = 0,$$

which induces

$$\lim_{k\to\infty} p\{G(k) \cap S_\varepsilon^* \neq \emptyset\} = 1 - \lim_{k\to\infty} p\{G(k) \cap S_\varepsilon^* = \emptyset\} = 1 - 0 = 1$$

that was to prove.

$\square$

**Remark 5.6.1.** *Since the probability that a random individual hits the optimal solution set with a positive measure is strictly positive, MDEA (in contrast to CDEA) complies with the assumptions of the theorem. This implies the global convergence of MDEA in probability.*

## 5.7 Probabilistic Convergence Analysis

The operations of algorithms CDEA and MDEA are relatively straightforward to describe (for details see Sections 5.3 and 5.5). On the other hand their exact theoretical analysis is relatively demanding and up to now not available in any publications. Nevertheless, the analysis of the role of random individuals in MDEA is relatively simple. By a random individual we mean a random point from the search space $S$. Since these random individuals form the part of the algorithm that ensures the asymptotic convergence to the global minimum of the cost function, it definitely has sense to have a clear idea about how this feature of MDEA works. That is the reason we focus in this part on the mechanism how random individuals contribute to the identification of the global minimum of the cost function.

From the description of CDEA and MDEA (see Section 5.3 pseudocode part (3)(a)(iv)) it is apparent that both algorithms are greedy in the following sense:

When they attain a point in the search space with a small value of the cost function they will not lose it unless they replace it by another point with even smaller value of the cost function.

This feature complements conveniently with the random sampling part in the MDEA (see Section 5.5 pseudocode part (3)(c)). The random sampling explores the search space and can be characterized by the fact that more random individuals provide more detailed exploration of the search space. Technically speaking, when performing a practical calculation, the random sampling can bring the MDEA close to the global or very low (acceptable) local minimum and the mechanism of the differential evolution ensures the effective convergence to this minimum.

### 5.7.1 Sampling of the Search Space by Random Individuals

Let us suppose we have somehow identified a local minimum of the cost function $F$ at the point $x_{\mathrm{L}}$ with the cost function value $F(x_{\mathrm{L}})$ (index L stands here for Local). We would like to try the possibility to find a better local minimum or preferably the global minimum of the cost function $F(x)$.

We make an assumption that there exists a part of the search space $S$ with cost function values lower than $F(x_{\mathrm{L}})$. We denote this region as the target region $\sigma$

$$\sigma = \{x \in S : F(x) < F(x_{\mathrm{L}})\}. \tag{5.6}$$

We denote the measure of the target region $\sigma$ as $\mu_0(\sigma)$. Additionally, we suppose $\mu_0(\sigma) > 0$. By the symbol $\mu(S)$ we understand the measure of the whole search space $S$. The target region $\sigma$ is thus the part of the search space $S$ that according to our assumption contains a minimum or minima with lower cost function values than $F(x_L)$.

Subsequently, we use the algorithm MDEA that includes the generation of random individuals, that is a random sampling. Now, we formulate a null hypothesis $H_0$. The hypothesis $H_0$ states that the probability $p$ to hit the target region with one random individual is $p = p_0$. The probability $p_0$ that we hit the target region $\sigma$ with one random individual is given by the ratio of $\mu_0(\sigma)$ and $\mu(S)$

$$p_0 = \frac{\mu_0(\sigma)}{\mu(S)}. \tag{5.7}$$

In this way the hypothesis $H_0$ determines the measure of the target region $\mu_0(\sigma)$ as well.

The hypothesis $H_0$ can be expressed symbolically as

$$H_0 : p = p_0, \tag{5.8}$$

where $p$ denotes the probability to hit the target region $\sigma$ with one random individual.

In principle, we can confirm or reject the hypothesis $H_0$ by generating a quantity of random individuals and monitoring whether some of them hit the target region $\sigma$ or not. The number $k$ of random individuals that should hit the target region $\sigma$ is described by the binomial distribution (see [2], page 140)

$$Bi(n, k, p_0) = \binom{n}{k} p_0^k (1 - p_0)^{n-k}. \tag{5.9}$$

After we generated $n$ random individuals there exist in principle two different results:

1. We got some individuals from the target region $\sigma$. This means we have found some points $x_{\mathrm{B}}$ with cost function values $F(x_{\mathrm{B}})$ lower than $F(x_{\mathrm{L}})$ (index B here stands for Better). This result is considered positive and we

can decide whether the lowest value of $F(x_B)$ is acceptable as a result of the optimization or whether to continue with the search for even better cost function values.

2. No random individuals hit the target region $\sigma$, that is we did not find any points $x_B$. What conclusion can we make based on this negative result? There are in principle three alternatives:

   • The target region $\sigma$ does not exists at all. This means that the point $x_L$ can be considered as a global minimum.

   • The target region $\sigma$ does exist but its measure $\mu(\sigma)$ is smaller than the supposed value $\mu_0(\sigma)$. This implies that the probability to hit the target region $\sigma$ with one random individual is smaller than $p_0$.

   • The target region $\sigma$ does exist and its measure $\mu_0(\sigma)$ is right but we did not hit it by accident, since we used exclusively random individuals that missed the target region.

The probability that the target region $\sigma$ should not be hit even once after generating $n$ random individuals is according to (5.9)

$$Bi(n, 0, p_0) = (1 - p_0)^n. \tag{5.10}$$

It is obvious that this probability converges to 0 with the increasing $n$ for $p_0 > 0$. Even if the random individuals indicate that the probability $p$ to hit the target region $\sigma$ is 0 or significantly smaller than the value $p_0$ we do not know this for sure, just because the generated individuals are random. We can claim this only with a relative certainty.

Now, it is suitable to utilize some terminology from the statistical hypotheses testing. It is necessary to set a fixed significance level $\alpha_S$. The quantity $\alpha_S$ represents the probability that we decline the hypothesis $H_0 : p = p_0$ although it is true

$$\alpha_S = P(H_0 \text{ true, but declined}), \tag{5.11}$$

where $P$ denotes the probability of the event.

The value of $\alpha_S$ depends on circumstances and in particular on the fact what quantity of risk to reject the right hypothesis is for us acceptable. It is usually chosen $0.05, 0.01, 0.005, \ldots$, but in fact it can be set arbitrarily. The significance

level $\alpha_S$ is sometimes called the error of the first kind in statistical hypotheses testing.

The logic of the hypotheses testing is that we determine some part of the binomial distribution $Bi(n, k, p_0)$ with a small probability $\alpha_S$ and declare this part of the distribution as critical. Since the probability $\alpha_S$ is small, it is relatively improbable that we hit the critical part. In our case the critical part corresponds to the "no hit of the target region $\sigma$" area that is to the result $Bi(n, 0, p_0)$. Since the value $Bi(n, 0, p_0)$ is according to (5.10) decreasing with increasing $n$ and $p_0 > 0$ we have to take the number $n$ in such a way that the result $Bi(n, 0, p_0)$ is a part of the binomial distribution $Bi(n, k, p_0)$ with probability equal to or less than $\alpha_S$.

Now, it is possible to determine the smallest such $n$ denoted by $n_0$. We calculate it from the equation

$$(1 - p_0)^{n_0} = \alpha_S$$

as the minimal number guaranteeing to attain the significance level $\alpha_S$ which gives

$$n_0 = \frac{\log(\alpha_S)}{\log(1 - p_0)}, \tag{5.12}$$

where $\log(x)$ stands for the decadic logarithm of a positive real number $x$.

From the considerations above it follows that if we generate $n \geq n_0$ random individuals and none of them hits the target region $\sigma$ we can claim that the probability $p$ to hit the target region $\sigma$ is $p < p_0$ only with the risk $\alpha_S$. We introduce finally the concept of the relative certainty $C_R$ (see Section 3.2.3 for more information) by the relation

$$C_R = 1 - \alpha_S.$$

Now, we can formulate the following proposition.

**Proposition 5.7.1.** *Let us assume that we generate at least $n = n_0$ random individuals, where $n_0$ is defined by the relation (5.12), and not even one hits the target region $\sigma$. Then we can claim with relative certainty at least $C_R = 1 - \alpha_S$ that the actual probability $p$ to hit the target region with one random individual is less than $p_0$. This also implies that the measure of the target region is smaller than $\mu_0(\sigma)$ with the same relative certainty $C_R$.*

**Proof:** The statement of the proposition follows easily from the meaning of the significance level $\alpha_S$ and the value $n_0$ given by the relation (5.12). Suppose we generated $n \geq n_0$ random individuals and not even one hits the target region $\sigma$. Since it definitely holds

$$n \geq n_0 = \frac{\log(\alpha_S)}{\log(1 - p_0)},$$

we have

$$n \log(1 - p_0) \leq n_0 \log(1 - p_0) = \log(\alpha_S),$$

which implies

$$(1 - p_0)^n \leq (1 - p_0)^{n_0} = \alpha_S.$$

The last relation expresses the fact that when the hypothesis $H_0$ is true then the probability that no random individual out of $n$ hits the target region $\sigma$ is smaller than $\alpha_S$. Since the value $\alpha_S$ is relatively small we declare this situation as relatively improbable and accept the risk $\alpha_S$ to decline the hypothesis $H_0$ with a relative certainty $C_R = 1 - \alpha_S$. In other words we say that since this situation is on the assumption $p = p_0$ relatively improbable its occurence is caused rather by the fact that $p < p_0$. $\qquad \square$

**Remark 5.7.1.** *It is apparent from the relation (5.12) that the number $n_0$ is dependent on the significance level $\alpha_S$ and on the assumed probability $p_0$.*

## 5.7.2 More Probabilistic Estimates

In spite of the fact that the formula (5.12) is relatively simple, it can be further simplified. Let us introduce an auxiliary quantity

$$\psi = np_0 \tag{5.13}$$

that expresses the relation between the number $n$ of generated random individuals and the assumed probability to hit the target region $p_0$ defined by (5.7). Now, we can express the probability that not even one random individual out of $n$ hits the target region $\sigma$ in the following way

$$(1 - p_0)^n = (1 - p_0)^{\frac{\psi}{p_0}} = \left[(1 - p_0)^{\frac{1}{p_0}}\right]^{\psi}.$$

When we again make use of the significance level $\alpha_S$ defined by the relation (5.11) we can write

$$\left[ (1 - p_0)^{\frac{1}{p_0}} \right]^{\psi} \leq \alpha_S.$$

Introducing the quantity $\psi_0$ as a minimal value of $\psi$ complying with the previous inequality, we get an equation

$$\left[ (1 - p_0)^{\frac{1}{p_0}} \right]^{\psi_0} = \alpha_S.$$

We need to estimate in a suitable way the term in the square brackets. The task can be reformulated in the following way: Find the supreme of the function

$$g : y = (1 - x)^{\frac{1}{x}}$$

with domain $D(g) = (0, 1)$. Elementary analysis gives us an estimation

$$(1 - p_0)^{\frac{1}{p_0}} \leq \frac{1}{e}.$$

Using this estimate gives

$$\left( \frac{1}{e} \right)^{\psi_0} = \alpha_S.$$

From this relation we immediately get

$$\psi_0 = -\ln(\alpha_S), \tag{5.14}$$

where $\ln(x)$ stands for the natural logarithm of the positive real number $x$. The quantity $\psi_0$ gives us a useful representation for the term

$$\psi_0 = N_0 p_0.$$

The last relation expresses the fact that when we assume the hypothesis $H_0 : p = p_0$ and no random individual hits the target region $\sigma$ we need to take $N_0$ in such a way that

$$N_0 p_0 \geq -\ln(\alpha_S)$$

to be entitled to claim that $H_0 : p = p_0$ does not hold implying $p < p_0$.

In case we need to express explicitly the number of individuals not hitting the target region $\sigma$ we can use the relation (5.13) and get

$$N_0 = -\frac{1}{p_0} \ln(\alpha_S). \tag{5.15}$$

Analogously to Proposition 5.7.1 we can state the following:

**Proposition 5.7.2.** *Let us assume we generate at least $n = N_0$ random individuals where $N_0$ is defined by the formula (5.15) and not even one individual hits the target region $\sigma$. Then we can claim with the relative certainty at least $C_R = 1 - \alpha_S$ that the actual probability $p$ to hit the target region is less than $p_0$.*

**Proof:** The proof follows from the preceding considerations.

**Remark 5.7.2.** *The principal advantage of the formula (5.15) over the formula (5.12) is the fact that in the former the dependence on the value $p_0$ is much simpler than in the latter. This is based on the fact that $\psi_0$ according to (5.14) does not depend on the value $p_0$ at all.*

To illustrate the dependence of the quantities $\psi_0$ and $N_0$ on values $\alpha_S$ for three different levels of the probability $p_0$ we summarized these quantities in Table 5.3. The Table 5.3 demonstrates the fact that when we suppose a fixed value of probability $p = p_0$ and perform $N_0$ experiments with a negative result we can claim with a relative certainty $C_R$ that $p < p_0$. The higher relative certainty we require the more experiments have to be performed, in other words the more random individuals have to be generated.

It is not complicated to verify that formulas (5.12) and (5.15) for the numbers $n_0$ and $N_0$ are equivalent under the condition $p_0 \ll 1$.

**Lemma 5.7.3.** *Formulas (5.12) for the value $n_0$ and (5.15) for the value $N_0$ are equivalent on the assumption $p_0 \ll 1$.*

**Proof:** The following formula holds for logarithms with different bases

$$\log_a(x) \cdot \log_b(a) = \log_b(x).$$

Using this formula in our context gives

$$\log_{10}(\alpha_S) \cdot \ln(10) = \ln(\alpha_S),$$

where $\ln(x)$ denotes the natural logarithm of a positive real number $x$. Substituting the last formula into the (5.12) gives

| $\alpha_S$ | $C_R$ | $\psi_0$ | $N_0$ | $N_0$ | $N_0$ |
| --- | --- | --- | --- | --- | --- |
| | | | $p_0 = 10^{-6}$ | $p_0 = 10^{-9}$ | $p_0 = 10^{-12}$ |
| 0.1 | 0.9 | 2.302 586 | 2 302 586 | 2 302 586 000 | 2 302 586 000 000 |
| 0.05 | 0.95 | 2.995 733 | 2 995 733 | 2 995 733 000 | 2 995 733 000 000 |
| 0.01 | 0.99 | 4.605 171 | 4 605 171 | 4 605 171 000 | 4 605 171 000 000 |
| 0.005 | 0.995 | 5.298 318 | 5 298 318 | 5 298 318 000 | 5 298 318 000 000 |
| 0.001 | 0.999 | 6.907 756 | 6 907 756 | 6 907 756 000 | 6 907 756 000 000 |
| 0.000 5 | 0.999 5 | 7.600 903 | 7 600 903 | 7 600 903 000 | 7 600 903 000 000 |
| 0.000 1 | 0.999 9 | 9.210 341 | 9 210 341 | 9 210 341 000 | 9 210 341 000 000 |
| 0.000 05 | 0.999 95 | 9.903 488 | 9 903 488 | 9 903 488 000 | 9 903 488 000 000 |
| 0.000 01 | 0.999 99 | 11.512 926 | 11 512 926 | 11 512 926 000 | 11 512 926 000 000 |
| 0.000 005 | 0.999 995 | 12.206 073 | 12 206 073 | 12 206 073 000 | 12 206 073 000 000 |
| 0.000 001 | 0.999 999 | 13.815 511 | 13 815 511 | 13 815 511 000 | 13 815 511 000 000 |

Table 5.3: Values of $\psi_0$ and $N_0$ for different levels of probability $p_0$ and different values $\alpha_S$

$$n_0 = \frac{\log(\alpha_S)}{\log(1 - p_0)} = \frac{\ln(\alpha_S)}{\log(1 - p_0) \cdot \ln(10)} = \frac{\ln(\alpha_S)}{\ln(1 - p_0)}.$$

Assuming $p_0 \ll 1$, we can approximate

$$\ln(1 - p_0) \approx -p_0.$$

Using the last approximation gives

$$n_0 \approx \frac{\ln(\alpha_S)}{-p_0)} = N_0,$$

which was to prove. $\qquad\square$

It is interesting to note that the Proposition 5.7.1 and its equivalent Proposition 5.7.2 can be reformulated in another rather unexpected way.

**Corollary 5.7.4.** *Let us assume that the probability $p$ to hit the target region $\sigma$ with one random individual is equal to $p_0$. When considering $n$ random individuals, we denote by $P_1$ the probability to hit the target region $\sigma$ with at least one individual. The probability $P_1$ is obviously*

$$P_1 = 1 - (1 - p_0)^n.$$

*When none of these $n$ random individuals hits the target region $\sigma$, we can claim with relative certainty $C_R = P_1$ that the probability $p < p_0$.*

**Proof:** The probability $P_0$ that none out of $n$ random individuals hits the target region $\sigma_0$ is apparently

$$P_0 = (1 - p_0)^n.$$

The probability $P_1$ is obviously given by

$$P_1 = 1 - P_0 = 1 - (1 - p_0)^n.$$

But by considerations in Proposition 5.7.1 we have $(1 - p_0)^n = \alpha_S$ and the relative certainty $C_R$ is given by $C_R = 1 - \alpha_S$ implying

$$C_R = P_1.$$

$\square$

**Remark 5.7.3.** *The conclusion $p < p_0$ obviously implies that the measure of the target region is smaller than $\mu_0(\sigma)$ in accordance with relation (5.7).*

## 5.8 Lipschitz Continuous Cost Functions

The Lipschitz continuity of the cost function is a prerequisite that makes the prospective of finding the global minimum of the cost function more realistic. It ensures that the cost function changes its values in a rather limited way and that its deep minima occupy relatively larger regions.

Additionally, it offers another possibility how to interpret the negative results in sampling the search space with random individuals. Since we know that the cost function does not change its values extremely rapidly, we can transform the estimates of the target region size into the lower estimate of the cost function value at the global minimum. In other words, if we found a local minimum of the cost function at the point $x_L$ and none of random individuals provides any result that is better than $F(x_L)$, we can claim that the lowest possible value of the cost function is limited from below by a certain value.

### 5.8.1 Lipschitz Continuity of the Cost Function

The Lipschitz continuity of a function can be defined in the following way:

**Definition 5.8.1.** *Let us have a function $F(x)$ with a domain $D$. We say that the function $F(x)$ is Lipschitz continuous on the domain $D$ if there exists a real constant $L > 0$ and for any two points $x_1, x_2$ from the domain $D$ the following relation holds:*

$$|F(x_1) - F(x_2)| \leq L \cdot \text{dist}(x_1, x_2). \tag{5.16}$$

The symbol $|x|$ denotes the usual absolute value of a real number $x$ and $L > 0$ is a constant (in this context called the Lipschitz constant). The term $\text{dist}(x_1, x_2)$ stands for a metrics of the domain $D$, in our case the usual Euclidean metrics in an $d$-dimensional Euclidean space which is defined as

$$\text{dist}(x_1, x_2) = \left[ \sum_{i=1}^{d} (x_{1i} - x_{2i})^2 \right]^{\frac{1}{2}}, \tag{5.17}$$

where $x_{1i}, x_{2i}$ are individual coordinates of points $x_1$ and $x_2$.

## 5.8.2 Consequences of the Lipschitz Continuity

Assuming that the cost function $F$ is Lipschitz continuous, we can further extend the results of Section 5.7. Thus, from now on we assume that the cost function $F(x)$ is Lipschitz continuous that is it complies with the requirement (5.16). We also suppose that the search space $S$ (which is the domain of the cost function $F(x)$) is a compact set. In Euclidean spaces this means that the search space $S$ is bounded and closed.

Based on these assumptions we get immediately the following statement.

**Proposition 5.8.1.** *When the search space $S$ is a compact set and the cost function $F(x)$ is Lipschitz continuous on $S$, then the cost function $F(x)$ has at least one global minimum.*

**Proof:** The Lipschitz continuity of the function $F$ implies its pointwise continuity. The statement of the proposition is then an easy consequence of the Weierstrass extreme value theorem of elementary analysis stating that any continuous function defined on a compact domain attains on this domain its extrema. □

When we generate $N_0$ random individuals ($N_0$ is defined by relation (5.15)) and none of them hits the target region $\sigma$ then we know according to Section 5.7 that with relative certainty $C_R$ the measure of the target region $\sigma$ is smaller that a given value $\mu_0$, where $\mu_0$ corresponds to a certain probability $p_0$ to hit the target region $\sigma$ with one random individual. In other words the value $\mu_0$ is an upper limit for the size of the target region $\sigma$

$$\mu_0 > \mu(\sigma). \tag{5.18}$$

The Lipschitz continuity of the cost function $F$ makes then possible to formulate the following statement.

**Proposition 5.8.2.** *Let us assume the following setting: We look for a global minimum of the Lipschitz continuous cost function $F(x)$ defined on the d-dimensional search space $S \subset \mathbb{R}^d$. We have identified a minimum of the cost function $F(x)$ at a point $x_L$ with the value $F(x_L)$. Further, we have generated more than $N_0$ random individuals from the search space $S$ (where $N_0$ is defined by the relation (5.15) ) and not even one attained a cost function value lower than $F(x_L)$. Then we can claim with a relative certainty $C_R = 1 - \alpha_S$ that the cost function values are limited from below by the value $F_M$, where*

$$F_{\mathrm{M}} = F(x_{\mathrm{L}}) - L \cdot \rho, \tag{5.19}$$

*where*

$$\rho = \left( \frac{d!! \cdot \mu_0}{2^{\lceil \frac{d}{2} \rceil} \cdot \pi^{\lfloor \frac{d}{2} \rfloor}} \right)^{\frac{1}{d}} \tag{5.20}$$

*and $L$ is the constant defining the Lipschitz continuity of the cost function $F(x)$ (see the relation (5.16)).*

**Proof:** According to our assumption we have generated $n$ random individuals, where $n > N_0 = -\frac{1}{p_0} \ln(\alpha_{\mathrm{S}})$. If we have no random individual $x$ with $F(x) < F(x_L)$ (no positive result), then according to the Proposition 5.7.2 we can claim with the relative certainty $C_{\mathrm{R}} = 1 - \alpha_{\mathrm{S}}$ that $p < p_0$ indicating that $\mu(\sigma) < \mu(\sigma_0) = \mu_0$. So, the value $\mu_0$ represent and an upper limit for the measure of the target region $\sigma$. Since the cost function $F(x)$ is Lipschitz continuous, there exists a certain limit concerning how deeply relatively to the value $F(x_{\mathrm{L}})$ the cost function $F(x)$ can go. This limit evidently depends on the shape of the target region $\sigma$ and is the biggest when the target region $\sigma$ is of spherical shape. In this case this limit achieves the value $L \cdot \rho$, where $\rho$ is the radius of the spherical target region. Since the volume of a ball in the $d$-dimensional Euclidean space is given by the formula (see (3.15)

$$V_d(R) = \frac{2^{\lceil \frac{d}{2} \rceil} \cdot \pi^{\lfloor \frac{d}{2} \rfloor}}{d!!} \cdot R^d,$$

where $R$ is the radius of the ball, we can put

$$\frac{2^{\lceil \frac{d}{2} \rceil} \cdot \pi^{\lfloor \frac{d}{2} \rfloor}}{d!!} \cdot \rho^d = \mu_0$$

to obtain the radius $\rho$. This equation implies

$$\rho = \left( \frac{d!! \cdot \mu_0}{2^{\lceil \frac{d}{2} \rceil} \cdot \pi^{\lfloor \frac{d}{2} \rfloor}} \right)^{\frac{1}{d}},$$

which is the relation (5.20).

The relation (5.19) is an obvious consequence of the Lipschitz continuity of the cost function $F(x)$.

$\square$

**An Example**

Let us illustrate the meaning of Proposition 5.8.2 on a simple example. We suppose three different values of the quantity $\mu_0 = \mu(\sigma_0) = p_0 \cdot \mu(S)$; $\mu_0 = 10^{-6}$, $\mu_0 = 10^{-9}$ and $\mu_0 = 10^{-12}$. We calculate the quantity $\rho$ for different dimension $d$ of the Euclidean space. The results are summarized in the Table 5.4.

| | $\rho$ | | |
|---|---|---|---|
| $d$ | $\mu_0 = 10^{-6}$ | $\mu_0 = 10^{-9}$ | $\mu_0 = 10^{-12}$ |
| 2 | $5.6419 \cdot 10^{-4}$ | $1.78412 \cdot 10^{-5}$ | $5.6419 \cdot 10^{-7}$ |
| 4 | 0.021217 | 0.003773 | $6.70938 \cdot 10^{-4}$ |
| 6 | 0.076053 | 0.024050 | 0.007605 |
| 8 | 0.149263 | 0.062944 | 0.026543 |
| 10 | 0.228741 | 0.114642 | 0.057457 |
| 12 | 0.308700 | 0.173595 | 0.097619 |
| 16 | 0.461605 | 0.299758 | 0.194657 |
| 20 | 0.601746 | 0.426004 | 0.301587 |
| 30 | 0.902212 | 0.716652 | 0.569257 |
| 40 | 1.151008 | 0.968452 | 0.814851 |
| 50 | 1.365331 | 1.189154 | 1.035710 |
| 60 | 1.555319 | 1.386179 | 1.235434 |
| 80 | 1.885040 | 1.729102 | 1.586064 |
| 100 | 2.168981 | 2.024211 | 1.889104 |

Table 5.4: Values of $\rho$ for different values of $\mu_0$ and different dimensions $d$

The numbers in the Table 5.4 illustrate the fact that the estimate (5.19), (5.20) works best for search spaces with small dimensions $d$. In this case it limits the value of the minimum of the cost function considerably more than in cases with the high dimension $d$. This fact is caused by the reality that in Euclidean

spaces of high dimension a ball with a small volume can have relatively large radius (compare the relation (3.17) for the asymptotic formula for the volume of ball in the $d$-dimensional Euclidean space).

# Chapter 6

# Models of Heat Conduction

It is possible to define several alternative mathematical models of heat conduction in three dimensional bodies that correspond to various physical situations. The principal quantity in each model is a temperature field. The temperature field is usually denoted as $T(x)$ for stationary models and $T(x,t)$ for nonstationary models. The symbol $x$ denotes an arbitrary point inside or on the surface of the body and $t$ stands for the time within a relevant time period. The temperature field describes how the temperature $T$ is distributed within the body.

An integral part of the model is represented by so called boundary conditions that model the heat transfer mechanisms on the surface of the body. Another important aspect of the model is an initial condition that determines the temperature field in the model at the beginning of the relevant time period. The initial condition applies of course only to nonstationary models.

Heat sources also play a significant role in the model. Heat sources represent mechanisms that generate heat leading to temperature increase. In principle, we can divide them into two kinds. Volume heat sources that generate heat inside the volume of the body. Surface heat sources on the other hand generate heat exclusively on the surface of the body. Typically, volume heat sources are represented by a term in the partial differential equation describing the model. Surface heat sources by contrast mostly constitute a part of the boundary condition.

Since we deal with radiation heating in this thesis, we concentrate now on the topic of the heat radiation.

## 6.1   Own Heat Radiation and the Stefan–Boltzmann Law

Hot bodies cool down not only because they are surrounded by colder environment. The also lose energy by their own heat radiation. Exemplary examples are stars that find themselves in practical vacuum but despite this fact they lose enormous amounts of energy by radiation.

Every body radiates electromagnetic energy. The quantity of this energy depends strongly on the absolute temperature of the body and also on its surface properties. Bodies in general are characterized by three mechanisms that describe their behaviour with respect to the incident radiation energy. These are absorption, reflectivity and transmission. The relation between these mechanisms is described by a simple relation (see [31])

$$\alpha_r + \rho_r + \tau_r = 1. \tag{6.1}$$

Here $\alpha_r$, $\rho_r$ and $\tau_r$ denote the coefficients of absorption, reflectivity and transmissivity respectively. The relation (6.1) expresses the fact that the incoming radiation energy is partly absorbed, partly reflected and the rest is transmitted through the body. When a body is in thermodynamic balance with its environment, then it radiates the same amount of energy as it absorbs from the incident radiation. A black body approximates the situation when all incident radiation energy is absorbed by the body.

That is why we introduce a notion of an ideal radiator (the perfect black body). Such a perfect black body absorbs all incoming radiation energy. This means that no radiation is reflected and no radiation is transmitted through the body ($\alpha_r = 1, \rho_r = 0, \tau_r = 0$). That is all incident radiation energy is transformed into the body's own heat radiation.

The Stefan-Boltzmann law describes quantitatively the power radiated by the black body due to its temperature. Specifically, the Stefan-Boltzmann law states that the total power emitted from a unit surface area of a black body is directly proportional to the fourth power of the black body's absolute temperature $T$. It is usually expressed is the form (see [42], page 320)

$$j = \sigma T^4,$$

where $j$ is the power radiated from a unit surface area, $\sigma$ stands for the Stefan–

Boltzmann constant and $T$ is the absolute temperature. The numerical value of $\sigma$ is $\sigma = 5.670 \cdot 10^{-8}$ Wm$^{-2}$K$^{-4}$.

It is interesting to note that the Stefan–Boltzmann constant can be derived theoretically from other fundamental physical constants (see [42]),

$$\sigma = \frac{2\pi^4 k_B^4}{15 c_0^2 h^3},$$

where $k_B$ is the Boltzmann constant, $k_B = 1.381 \cdot 10^{-23}$ JK$^{-1}$, $h$ denotes the Planck constant, $h = 6.626 \cdot 10^{-34}$ Js, and $c_0$ stands for the speed of light in vacuum, $c_0 = 2.998 \cdot 10^8$ ms$^{-1}$.

Bodies that do not absorb all incident radiation are called grey bodies. They emit less total energy compared to black bodies. This fact is characterized by a parameter called emissivity $\varepsilon$ ($0 < \varepsilon < 1$). For grey bodies the Stefann-Boltzmann law has the form

$$j = \varepsilon \sigma T^4.$$

Max Planck formulated in 1900 the relation for the intensity of the monochromatic temperature radiation of the black body. This formula describes quantitatively how the radiated energy is distributed between various wave lengths in dependence on the absolute temperature of the black body (see [31])

$$E(\lambda) = \frac{2\pi h c_0^2}{\lambda^5 \left(e^{\frac{hc_0}{k_B T \lambda}} - 1\right)}. \tag{6.2}$$

Here $E(\lambda)$ denotes the energy radiated on the wave length $\lambda$ and $T$ is the absolute temperature. The Planck law (6.2) is illustrated by the Figure 6.1. It is interesting to note that the Planck formula (6.2) is one of the milestones marking the twilight of the classical physics, since it was deduced on the assumption that energy is not a continuous quantity and can be released only in discontinuous amounts called energy quanta (for details see [3]).

## 6.2   Heat Equation

Let us consider a bounded body $\Omega \subset \mathbb{R}^3$ with Lipschitz continuous boundary $\Gamma = \partial\Omega$ (see Definition 3.1.6). It is possible to introduce the following general model described by a parabolic partial differential equation of the second order
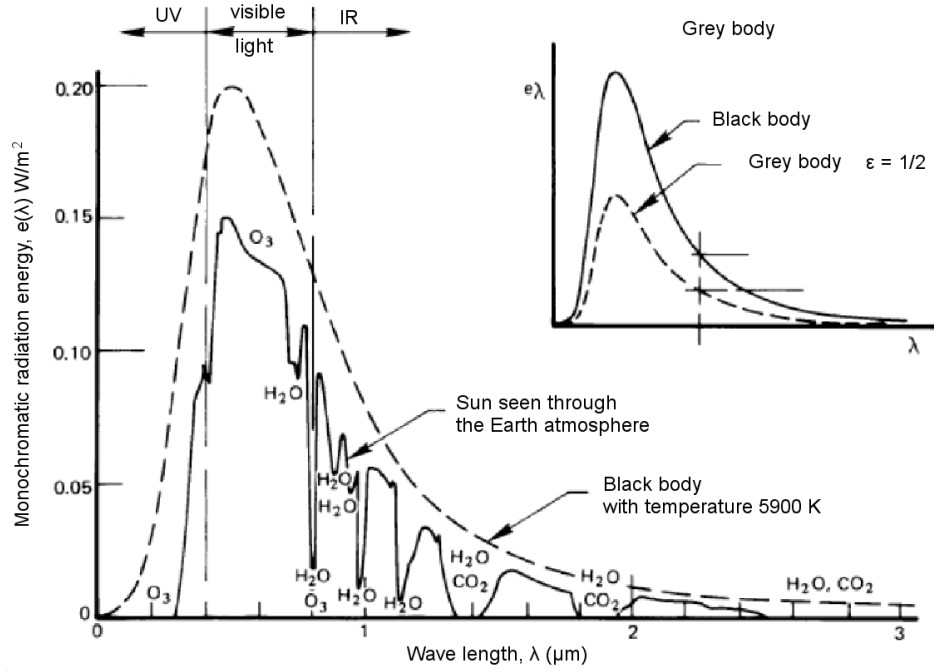
Figure 6.1: Illustration of the Planck law for the black, grey and real bodies

$$c(x)\rho(x)\frac{\partial T(x,t)}{\partial t} - \nabla \cdot (\hat{\lambda}(x)\nabla T(x,t)) = Q(x,t). \qquad (6.3)$$

The function $T(x,t)$ denotes the temperature field we want to determine, the symbol $\frac{\partial T(x,t)}{\partial t}$ represents the partial derivative of the temperature field according to the time $t$, the point $x = (x_1, x_2, x_3) \in \Omega$, $t \in (0, \tau)$, where $\tau$ is the total time during which we investigate the temperature field. The quantities $c(x)$ and $\rho(x)$ represent the specific heat of the body material at a steady pressure and material density, respectively. The symbol $\nabla$ denotes the vector Hamilton operator that can be expressed as

$$\nabla = \left(\frac{\partial}{\partial x}, \frac{\partial}{\partial y}, \frac{\partial}{\partial z}\right)$$

in Cartesian coordinates.

The quantity $\hat{\lambda}(x)$ is a tensor of the heat conductivity which is in a general case a tensor field of the second order. Material properties are in general dependent on the position in the body.

With respect to the fact that the shell mould are produced of a homogeneous and isotropic metal, we can consider the quantities $c(x)$, $\rho(x)$, and $\lambda(x)$ as mate-

rial constants $c$, $\rho$, and $\lambda$. Then it is possible to rewrite the equation (6.3) in the following way

$$c\rho\frac{\partial T(x,t)}{\partial t} - \lambda\Delta T(x,t) = Q(x,t), \qquad (6.4)$$

where the symbol $\Delta$ denotes the Laplace operator with respect to the space variables. That is in the Cartesian coordinates

$$\Delta T(x,t) = \sum_{i=1}^{3} \frac{\partial^2 T(x,t)}{\partial x_i^2},$$

where the symbol $\frac{\partial^2 T(x,t)}{\partial x_i^2}$ denotes the second derivative of the function $T(x,t)$ with respect to the corresponding space variable.

There are no volume heat sources in $\Omega$ in our case the body is heated exclusively by infrared heaters. Therefore, we can put $Q(x,t) = 0$ in (6.4) and write the equation in the form

$$\frac{\partial T(x,t)}{\partial t} = \Lambda\Delta T(x,t), \qquad (6.5)$$

where $\Lambda = \frac{\lambda}{c\rho}$ is a coefficient of the thermal conductivity.
As an initial condition we use

$$T(x,0) = T_0 \quad \text{in} \quad \Omega, \qquad (6.6)$$

where $T_0$ denotes the initial temperature of the body.

**Boundary Conditions**

We can use a Newton boundary condition for the considered model of the temperature field. The Newton boundary condition describes best the situation when the body is surrounded by air and heat transfer between the body and air takes place by the mechanism of heat convection. The Newton boundary condition can be defined in the form

$$\lambda\frac{\partial T(x,t)}{\partial n} = -\alpha(T(x,t) - T_{\text{air}}) + I(x) \qquad (6.7)$$

for the heated side of the body $\Omega$ and

$$\lambda\frac{\partial T(x,t)}{\partial n} = -\alpha(T(x,t) - T_{\text{air}}) \qquad (6.8)$$

for the rest of the body surface.  Here the symbol $\alpha$ denotes the coefficient of the heat transfer between the material of the body and air, $T_\text{air}$ stands for the temperature of the surrounding air and $n$ is a unit vector of the outer normal. The symbol $\frac{\partial T(x,t)}{\partial n}$ means the derivative of the temperature field according to the outer normal $n$.  The quantity $I(x)$ represents intensity of the radiation heating at a point $x$ on the heated part of the surface $\Gamma$.

The model with the Newton boundary condition is linear concerning the differential equation as well as the boundary condition.  This implies a linearity of the model as a whole, which is an advantage from the theoretical point of view as well as with respect to the complexity of computations based on this model.

**Own Heat Radiation**

The above mentioned Newton boundary condition can be further approximated to the physical reality by introduction another term representing the own temperature radiation of the body according to the Stefan–Boltzmann law.  The own heat radiation is strongly dependent on the temperature of the body, it is proportional to the fourth power of the absolute temperature.  On the hand the mould receives heat energy by radiation not only from infrared heaters but also from all bodies in the vicinity of the mould.  It is natural to put the temperature of these bodies equal to the temperature of air $T_\text{air}$.

In this case the boundary condition (6.7) and (6.8) are modified in the following way (see [5])

$$\lambda\frac{\partial T(x,t)}{\partial n} = -\alpha(T(x,t) - T_\text{air}) - \varepsilon\sigma(T^4(x,t) - T_\text{air}^4) + I(x) \qquad (6.9)$$

and

$$\lambda\frac{\partial T(x,t)}{\partial n} = -\alpha(T(x,t) - T_\text{air}) - \varepsilon\sigma(T^4(x,t) - T_\text{air}^4). \qquad (6.10)$$

Here the symbol $\varepsilon$ denotes emissivity of the mould and $\sigma$ is the Stefan–Boltzmann constant, $\sigma = 5.670 \cdot 10^{-8}$ Wm$^{-2}$K$^{-4}$.  The boundary conditions (6.9) and (6.10) are not linear which means that the whole model is nonlinear.  Neglecting the mechanism of own heat radiation leads to higher temperatures of the mould compared with reality.

## 6.3 Weak Formulation of the Stationary Heat Conduction

In this part we concentrate on the weak formulation of the stationary heat conduction task with Newton boundary conditions. We look for a function $u(x)$ satisfying the elliptic partial differential equation

$$\Delta u(x) = 0 \quad \text{in} \quad \Omega, \tag{6.11}$$

$$\frac{\partial u(x)}{\partial n} = -\alpha u(x) \quad \text{on} \quad \Gamma_0, \tag{6.12}$$

$$\frac{\partial u(x)}{\partial n} = I(x) - \alpha u(x) \quad \text{on} \quad \Gamma_H. \tag{6.13}$$

The symbol $\frac{\partial u(x)}{\partial n}$ denotes the derivative of the solution $u(x)$ with respect to the outer normal. The symbol $\alpha \geq \alpha_0 > 0$ stands for the coefficient of the heat transfer between the mould material and air, $I(x)$ is the intensity of the radiation heating. The symbol $\Gamma_0$ denotes the nonheated side of the mould, $\Gamma_H$ stands for the heated side of the mould. Naturally, it holds $\Gamma = \Gamma_0 \cup \Gamma_H$. We assume that the solution $u(x)$ is an element of the Hilbert space $H^1(\Omega)$.

Now, we use the standard procedure to obtain the weak formulation of the problem (6.11) – (6.13). We take a function $v \in H^1(\Omega)$ as a test function, multiply the equation (6.11) by $v$ and integrate over the volume $\Omega$. We get

$$\int_\Omega (\Delta u(x)) v \, dV = 0.$$

Multiplying by $-1$ and using the Green theorem (see the Theorem 3.1.5) implies

$$\int_\Omega \nabla u(x).\nabla v \, dV - \int_\Gamma \frac{\partial u(x)}{\partial n} v \, dS = 0.$$

By substituting for the term $\frac{\partial u(x)}{\partial n}$ from the relations (6.12) and (6.13), we obtain

$$\int_\Omega \nabla u(x).\nabla v \, dV \alpha \int_\Gamma u(x) v \, dS = \int_{\Gamma_H} I v \, dS.$$

The last integral relation can be written in the form

$$a(u, v) = b(v).$$

The bilinear form $a(\cdot, \cdot)$ and the functional $b(\cdot)$ satisfy the assumptions of the Lax–Milgram lemma. This gives the existence and uniqueness of the solution $u(x)$.

## 6.4    Weak Formulation of the Nonstationary Heat Conduction

In this part we focus on the weak formulation of the nonstationary heat conduction task with Newton boundary conditions (6.7) and (6.8). We look for a function $u(x, t)$ satisfying a parabolic partial differential equation with an initial condition and Newton boundary conditions. The boundary conditions are different for the heated side of the mould $\Gamma_H$ and nonheated side of the mould $\Gamma_0$.

The classical formulation of the task can be expressed by the following relations

$$\frac{\partial u(x, t)}{\partial t} = \Lambda \Delta u(x, t) \quad \text{in} \quad \Omega \times (0, \tau), \tag{6.14}$$

$$u(x, 0) = u_0(x) \quad \text{in} \quad \Omega, \tag{6.15}$$

$$\frac{\partial u(x, t)}{\partial n} = -\alpha u(x, t) \quad \text{on} \quad \Gamma_0 \times (0, \tau), \tag{6.16}$$

$$\frac{\partial u(x, t)}{\partial n} = I(x) - \alpha u(x, t) \quad \text{on} \quad \Gamma_H \times (0, \tau). \tag{6.17}$$

The symbols $\frac{\partial u(x,t)}{\partial t}$ and $\frac{\partial u(x,t)}{\partial n}$ denote the derivative of the solution $u(x, t)$ according to the time $t$ or according to the outer normal $n$, respectively. The term $u_0(x)$ represents the initial condition, $\Lambda$ stands for the coefficient of the thermal conductivity, $\alpha \geq \alpha_0 > 0$ denotes the coefficient of the heat transfer between the mould material and air, $I(x)$ is the intensity of the radiation heating. The symbol $\Gamma_0$ denotes the nonheated side of the mould, $\Gamma_H$ stands for the heated side of the mould. Naturally, it holds $\Gamma = \Gamma_0 \cup \Gamma_H$. Finally, $(0, \tau)$ is the relevant time interval in which we look for the solution $u(x, t)$.

The equation (6.14) is the differential equation describing the nonstationary task, the relation (6.15) represents the initial condition, the relation (6.16) is the

boundary condition for the nonheated side of the mould $\Gamma_0$, the relation (6.17) is the boundary condition for the heated side of the mould $\Gamma_H$.

The expression for the weak solution of the task (6.14) – (6.17) can be obtained by the standard procedure. We utilize test functions $v$ from the test space $V = H^1(\Omega)$, where $H^1(\Omega)$ is the corresponding Sobolev space. We can construct the solution $u(x, t)$ as a mapping $u(t)$ that to each $t \in (0, \tau)$ assigns a function $u(x)$ from $H^1(\Omega)$. This means that $u(t)$ represents the generalized function with the domain $(0, \tau)$ and range a part of the space $H^1(\Omega)$.

When we multiply the equation (6.14) by a test function $v$ and subsequently integrate over $\Omega$, we get

$$\int_\Omega \frac{\mathrm{d}u(t)}{\mathrm{d}t} v \, \mathrm{d}V = \Lambda \int_\Omega (\Delta u(t)) v \, \mathrm{d}V.$$

Since $u(t)$ are elements of the space $H^1(\Omega)$, the time derivative $\frac{\mathrm{d}u(t)}{\mathrm{d}t}$ also belongs to the space $H^1(\Omega)$. Using the Green's formula (see Theorem 3.1.5) gives

$$\frac{1}{\Lambda} \int_\Omega \frac{\mathrm{d}u(t)}{\mathrm{d}t} v \, \mathrm{d}V + \int_\Omega \nabla u(t).\nabla v \, \mathrm{d}V = \int_\Gamma \frac{\partial u(t)}{\partial n} v \, \mathrm{d}S.$$

By substituting for the term $\frac{\partial u(t)}{\partial n}$ from the boundary conditions (6.16) and (6.17) we obtain an integral identity

$$\frac{1}{\Lambda} \frac{\mathrm{d}}{\mathrm{d}t} \int_\Omega u(t) v \, \mathrm{d}V + \int_\Omega \nabla u(t).\nabla v \, \mathrm{d}V + \alpha \int_\Gamma u(t) v \, \mathrm{d}S = \int_{\Gamma_H} I(x) v \, \mathrm{d}S$$

that can be rewritten as

$$\frac{1}{\Lambda} \frac{\mathrm{d}}{\mathrm{d}t} \int_\Omega u(t) v \, \mathrm{d}V + \int_\Omega \nabla u(t).\nabla v \, \mathrm{d}V + \alpha \int_\Gamma u(t) v \, \mathrm{d}S = \int_{\Gamma_H} I(x) v \, \mathrm{d}S.$$

Finally, we can write

$$\frac{1}{\Lambda} \frac{\mathrm{d}}{\mathrm{d}t} (u(t), v) + a(u(t), v) = \langle I, v \rangle, \tag{6.18}$$

where

$$(u(t), v) = \int_\Omega u(t) v \, \mathrm{d}V,$$

$$a(u(t), v) = \int_\Omega \nabla u(t).\nabla v \, \mathrm{d}V + \alpha \int_\Gamma u(t) v \, \mathrm{d}S$$

and

$$\langle I, v \rangle = \int_{(\Gamma_H)} I(x) v \, \mathrm{d}S.$$

The equation (6.18) represents a weak formulation of the problem (6.14) – (6.17).

The weak solution corresponding to the weak formulation (6.18) is investigated in full detail in [37]. Existence and uniqueness of the weak solution is guaranteed by Proposition 11.1. Nevertheless, this proposition assumes simplified initial and boundary conditions; specifically, zero initial condition and homogeneous boundary conditions.

The case with a nonzero initial condition is also solved in [37] by Propositions 13.1., 13.2. and 13.3. Nonhomogeneous boundary conditions are considered in Propositions 13.8., 13.9. and 13.10.

The solution of the general problem can then be obtained as a composition of three partial solutions specified by Propositions 11.1., 13.1., 13.2. and 13.8 in [37]. This procedure is based on the linearity of the problem and cannot be in general used for a problem containing any type of nonlinearity.

Useful introductory information on solving nonlinear problems can be found in article [9]. Regarding nonlinear problems with nonlinearity in the boundary conditions only partial results were up to now achieved. See for instance the articles [16], [17], and [7], where the nonlinear boundary condition is studied for a stationary heat conduction task, and [8], where a nonstationary task in a 2-dimensional domain is investigated. In general, nonlinearities in the area of partial differential equations can be of different kinds and they may require various specialized methods for solving. For an extensive information in this respect see monographs [44] – [48].

# Chapter 7

# Numerical Results

This part describes the specific techniques and parameters used to optimize the infrared heating of a test mould. The target is to attain a uniform temperature field within the temperature range 255 – 265 °C on the working side of the mould, where the plastic leather is formed. We can come out from the usual assumption that a uniform heating generates a uniform temperature field. This assumption is here justified, because we deal with a shell mould of the uniform thickness and with homogeneous material and surface parameters.

The optimized positioning of infrared heaters over the mould and the corresponding heat flux incident onto the heated side of the mould is subsequently used as an input quantity for the modelling of the temperature field inside the mould. Specifically, the optimized heat flux forms a part of the boundary condition on the heated side of the mould according to the relation (6.9).

## 7.1 Optimization of Infrared Heaters Positioning

In this section we present the numerical optimization of the infrared heaters positioning over the mould. The optimization is realized for the mould shown in Figure 7.1. The dimensions of the mould are $0.8\,\mathrm{m} \times 0.4\,\mathrm{m} \times 0.15\,\mathrm{m}$. The thickness of the mould is $8\,\mathrm{mm}$.

The mould is divided into 2064 elementary triangles. Each triagle is described by 6 quantities according to the relation (4.2). The mould is heated up by 16 infrared heaters of the type Phillips with the heating power $1000\,\mathrm{W}$ (see Figure
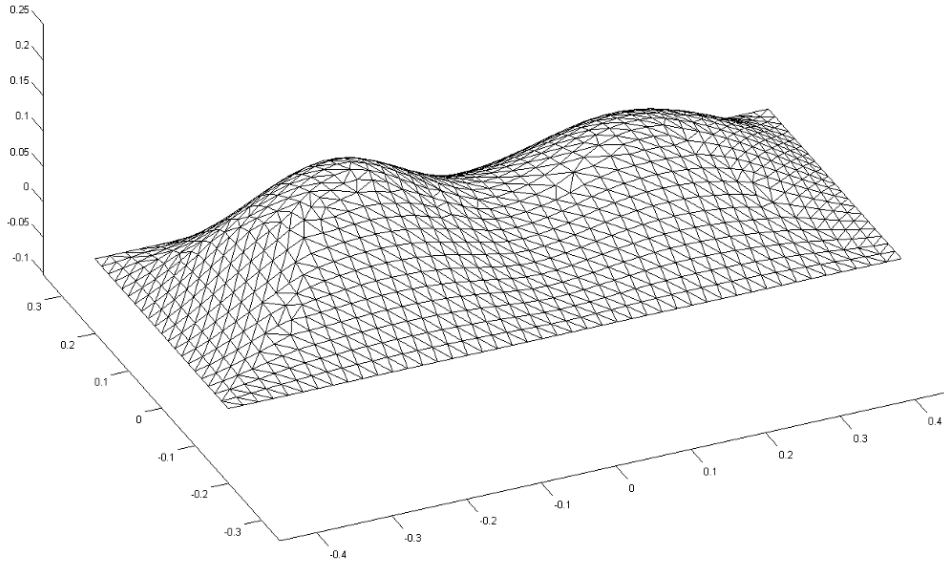
Figure 7.1: Shell mould to be heated by the set of 16 infrared heaters

2.2). The heaters are of a tubular shape and they are equipped with a mirror that reflects the heat radiation into the required direction. The length of the heater is 150 mm, width 40 mm. Each heater is characterized by six parameters according to the relation (4.1).

The initial setting of the infrared heaters is shown in Figure 7.2. The heaters are located in a horizontal plane 0.1 m above the mould highest point and they form a $4 \times 4$ equidistant array. This initial setting generates a corresponding heat flux on the heated side of the mould. The initial heat flux is also illustrated in Figure 7.2, where the heat flux in kW/m$^2$ incident at each elementary triangle is represented by different colour shades (see the legend of Figure 7.2).

We used the MDEA algorithm to optimize the heaters setting over the mould to obtain a uniform infrared heating. The parameters of the algorithm are:

Number of generations $NG = 8000$
Number of individuals $NP = 192$
Crossover probability $CR = 0.98$
Mutation factor $F = 0.6$
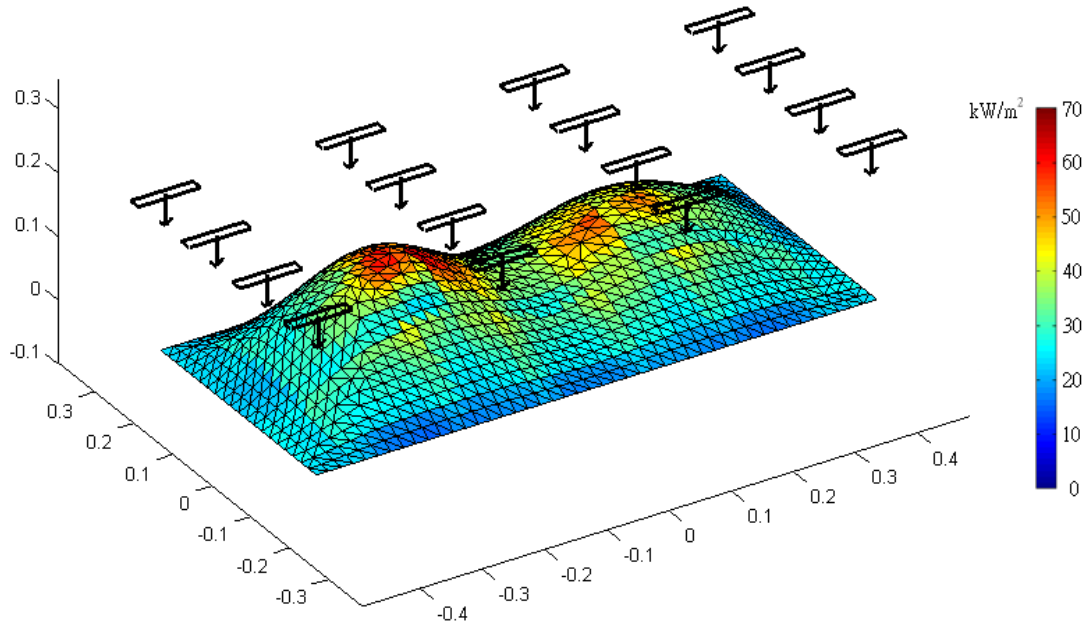Ratio of random individuals $R = 0.1$

Figure 7.2: The initial setting of infrared heaters above the mould including the heat flux generated on the upper side of the mould in kW/m²

To be able to start the algorithm, we need to create the first generation. This first generation is formed by a suitable randomization of the initial setting presented in Figure 7.2. Specifically, each infrared heater is moved randomly by a certain quantity from its initial position. The random change is also applied to the space orientation of the infrared heater. In this way all individuals in the first generation of the algorithm are created. Then the algorithm starts its standard operation as described in Sections 5.3 and 5.5.

During the operation of the algorithm it is necessary to deal with some special conditions. Since the heaters have finite dimensions it is possible that two or more heaters (as a part of one individual) collide or that a heater is too close to another heater or to the heated mould. Such individuals can be declared as illegal, expelled from the current generation and replaced by a legal individual. We used a different approach when these individuals are not expelled but only penalized. The cost function value of such an individual was raised by a certain quantity according to the collision degree.

Another anomalous state occurs when a part of an individual goes out of the prescribed domain. For instance when the centre of a heater is outside the prescribed region above the mould. To solve this situation we designed a so called

Bounce Back mechanism. The component of the individual out of its domain is reflected back into its domain and other components remain the same.

During the operation of the MDEA algorithm the value of the cost function of the best individual systematically decreases with the increasing number of generations. The decrease is extrememly rapid during first generations and successively approximates a limit value. In our case the starting value of the cost function was $F(y_0) = 20.3435$ and the final value after 8000 generations amounted to $F(y_{opt}) = 2.0201$. The value of the cost function in dependence on the generation number is displayed in Figure 7.3.
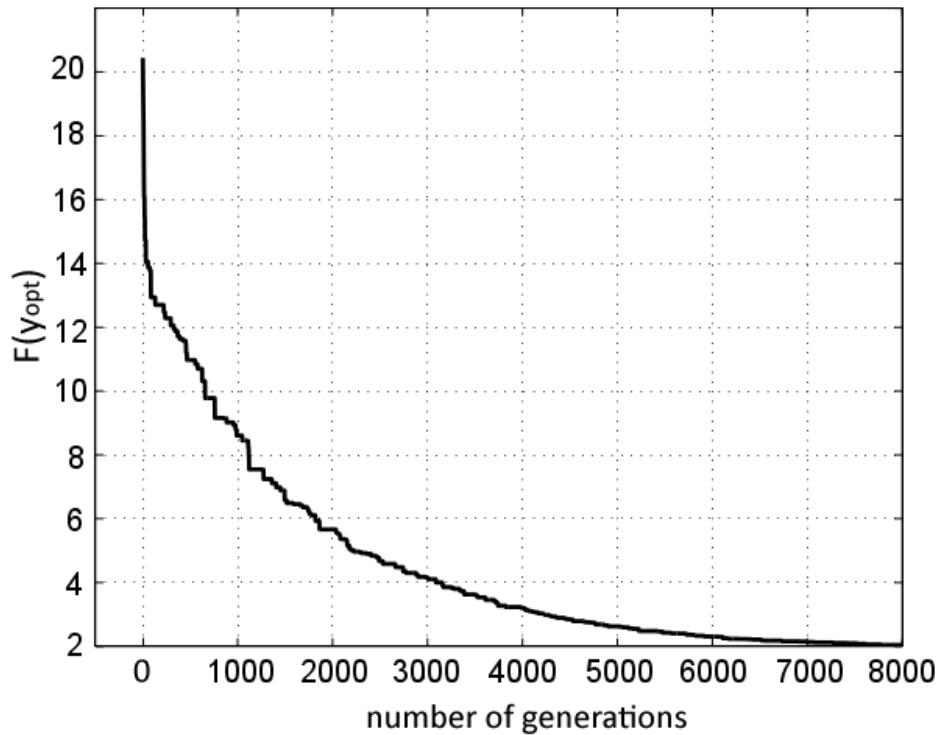


Figure 7.3: The value of the cost function during the MDEA operation

The optimization procedure realized by the MDEA provides the optimized positions and orientations of all 16 infrared heaters and the corresponding intensities of the radiation heat flux incident on individual elementary triangles of the mould. The time of calculation attained $26496\,\mathrm{s}$ which is almost 8.5 hours. Hardware specification: CPU IntelCore i7-3770, 3.4 GHz, 4 cores, RAM 32 GB.
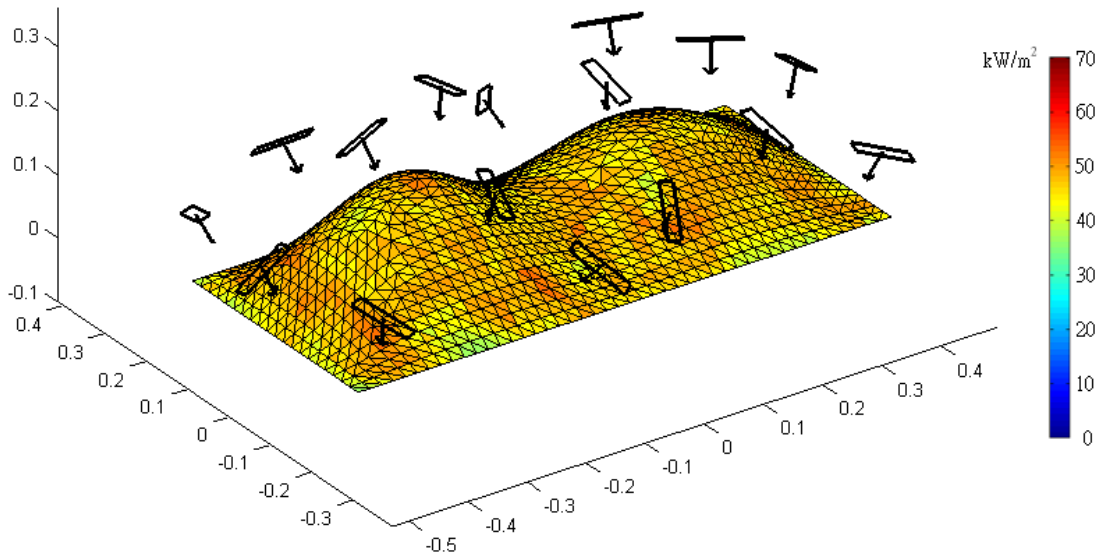
Figure 7.4: The optimized setting of infrared heaters above the mould including the heat flux generated on the upper side of the mould in kW/m²

## 7.2   Temperature Modelling

The modelling of the temperature field in the mould is based on the parabolic equation (6.5), initial condition (6.6), and boundary conditions (6.9) and (6.10). There are no volume heat sources in the mould. The radiation heat flux corresponding to the optimized positioning of the 16 infrared heaters is used as a surface heat source. Technically, it forms a part of the boundary condition (6.9). The boundary conditions also include cooling down by air around the mould and own heat radiation of the mould according to the Stefan–Boltzmann law.

The numerical calculation was realized by means of the programme package ANSYS 15.0.7. The calculation model includes the geometry of the mould and physical parameters of the mould material. We assume the temperature of the surrounding air $T_{\text{air}} = 22°$C, which is also the initial temperature of the mould $T_0 = 22°$C. The modelling itself takes place in the system ANSYS Mechanical. The used finite elements according to the ANSYS specification are Solid90 and Surf152.

The mould material parameters are:

- Mould material: Aluminium alloy

- Density: $\rho = 2770 \, \text{kg m}^{-3}$

- Specific heat: $c = 875\,\mathrm{J\,kg^{-1}K^{-1}}$

- Coefficient of the heat transfer between mould material and air: $\alpha = 20\,\mathrm{Wm^{-2}}$

- Heat conductivity $\lambda$: dependent on temperature ($148.62\,\mathrm{Wm^{-1}K^{-1}}$ at 22°C, $165\,\mathrm{Wm^{-1}K^{-1}}$ at 100°C, $175\,\mathrm{Wm^{-1}K^{-1}}$ at 200°C and higher

- Emissivity of the mould: $\varepsilon = 0.75$

- Time period: $\tau = 180\,\mathrm{s}$

The modelling of the temperature field was realized for three different alternatives of the infrared heating.

1. The initial positioning of the heaters in the horizontal plane and equidistant array shown in Figure 7.2.

2. The optimized positioning of infrared heaters by means of the MDEA algorithm illustrated in Figure 7.4.

3. The ideal absolutely uniform heating with the constant heat flux $47\,\mathrm{kW/m^2}$.

The resulting temperature field on the working side of the mould is represented in Figure 7.5 for the initial positioning of the heaters, in Figure 7.6 for the optimized positioning of heaters, and in Figure 7.7 for the ideal heating with the uniform heat flux $47\,\mathrm{kW/m^2}$. It should be noted that the colour shades correspond to a different scaling in each picture.

From Figure 7.5 it follows that the initial setting of heaters generates a temperature field that is mostly inhomogeneous. The temperature differences attain as much as $130\,°C$. Of course this is what we expected because in this case no optimization of the heaters positioning took place. The resulting temperature field serves exclusively for the comparison with the optimized state.

Figure 7.6 confirms that the optimized heaters positioning generates a relatively uniform temperature field on the working side of the mould. The maximal temperature difference is $13.5\,°C$, which is an acceptable uniformity level for the Slush Moulding technology.

Figure 7.7 demonstrates the temperature field corresponding to the ideally uniform heating which is not attainable by any real heating technology. Nevertheless, the maximal temperature difference is almost $8\,°C$.
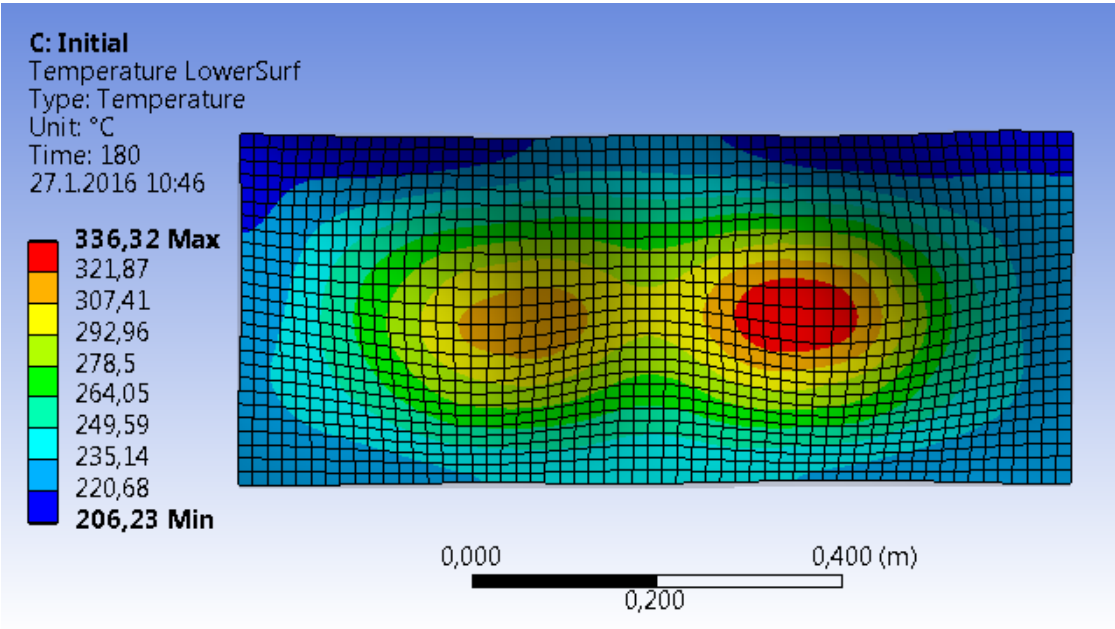
Figure 7.5: The temperature on the working side of the mould in °C for the initial positioning of the infrared heaters after 180 s of the heating
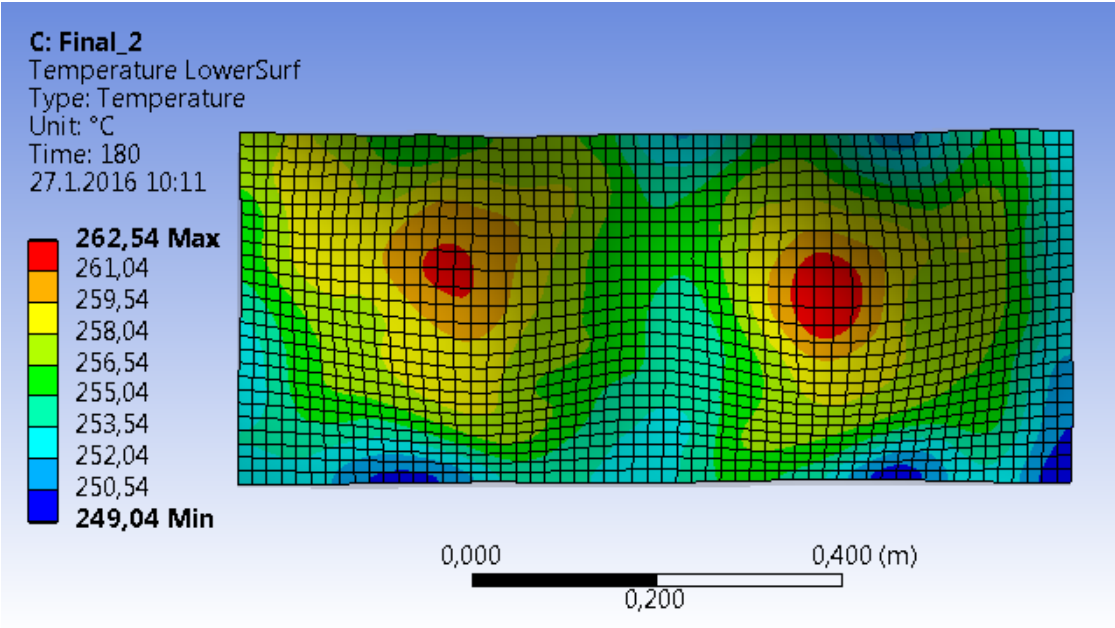


Figure 7.6: The temperature on the working side of the mould in °C for the optimized positioning of the infrared heaters after 180 s of the heating
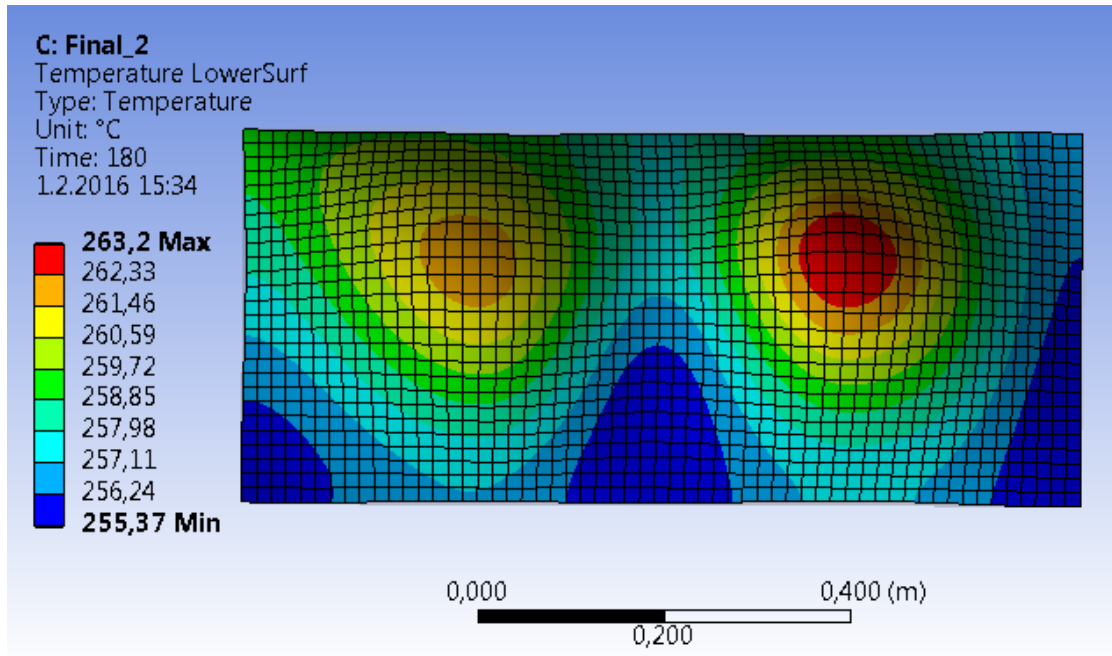
Figure 7.7: The temperature on the working side of the mould in °C for the absolutely uniform heating flux $47\,\text{kW/m}^2$ after 180 s of the heating

If we use Figure 7.7 as a reference and compare the maximal temperature differences for the optimized and ideal heating we come to a conclusion that the temperature difference $8\,°\text{C}$ is caused exclusively by the geometry of the mould and cannot be removed by any optimization. It remains only a rest of approximately $5.5\,°\text{C}$ that is connected with deficiencies in the optimized heating.

Even this nonuniformity of the temperature field could be in principle reduced by using more infrared heaters that would be placed in bigger distances from the heated side of the mould. Nevertheless, such a solution leads to higher energy consumption which is mostly not feasible from the cost effectiveness point of view.

# 7.3 Optimization of a System with Equivalent Components

Optimization tasks typically have several up to several tens of optimized parameters. The difficulty of the optimization increases with the number of these parameters. The parameters represent variables in the search space $S$ that has to be explored with the target to find the optimized minimum of the cost function. This means that each parameter corresponds to one dimension of the search space $S$.

Roughly speaking, we can say that the size of the search space $S$ exponentially increases with its dimension $d$. To illustrate this fact let us suppose that we have a problem with $d$ optimized parameters (variables) and the range of each variable is $\rho_{\text{var}}$. Then the measure of the search space $S$ amounts to

$$\mu(S) = \rho_{\text{var}}^d.$$

For $\rho_{\text{var}} > 1$ we get the exponential increase. This implies that to optimize problems with tens of parameters is a demanding task because we explore a search space $S$ that can be extremely huge and we look for a small part of it (the immediate neighbourhood of the optimized minimum).

Nevertheless, high numbers of optimized parameters are often caused by the situation when the optimized system includes several identical parts. The infrared heating optimization described in this doctoral thesis is a typical example. Each heater is represented by 6 parameters which means that for 16 heaters we have a search space $S$ with the dimension $d = 96$.

On the other hand the heaters are identical. This means that a specific numbering of heaters is not physically important. The heaters can be interchanged without any physical impact on the generated radiation heat flux. It follows that to any specific physical setting there exist in the search space $S$ 16! distinct states that differ only by a renumbering of the heaters.

Suppose now that the task has one optimal heaters positioning. Then in terms of the search space $S$ this optimal positioning corresponds to 16! of global minima of the cost function defined in $S$. This of course applies to any specific setting of the infrared heaters, in particular to any potential local minimum of the cost function. This implies that each local minimum of the cost function has in the search space $S$ 16! of "equivalent" local minima with the same value of

the cost function.

To conclude, we remind that $16! \doteq 2.0923 \cdot 10^{23}$ which is considerably more than the number of people on the Earth ($\sim 10^{10}$) or stars in the Gallaxy ($\sim 10^{11}$). This provides the reader with an approximate idea about complexity of the search space $S$ corresponding to a relatively common optimization task.

# Chapter 8

# Conclusions

In this doctoral thesis we solve an interconnected problem of the infrared heating of the shell metal mould and the subsequent modelling of the temperature field in the mould body.

The heating of the mould is realized by a system of 16 infrared heaters. However, the generalization to any number of heaters is quite obvious. Because the shell mould is potentially of complicated shape and the number of heaters is relatively high, the task of positioning the heaters over the mould is hardly solvable by any analytic method.

Therefore, the problem was reformulated as an optimization task. The cost function of the task evaluates the measure of deviation from the required heating. Even so, this optimization task is beyond reach of standard optimization techniques. This is because the cost function might have extremely many local minima. This fact implies that for instance gradient methods would end up at a local minimum and their result would be strongly dependent on the starting point of the optimization. This was the reason we started experimenting with evolutionary computing methods. These techniques include genetic algorithms and differential evolution algorithms. Finally, the differential evolution algorithms proved best to solve the optimization task.

Nevertheless, during the use and study of differential evolution algorithms we revealed principle limitations of the standard differential evolution algorithms. The principle weakness of the CDEA algorithm is a possible premature convergence of the computing process to a local minimum of the cost function. This fact was the reason for a search of an improved algorithm that could provide better results regarding the convergence to the global minimum of the cost function.

The MDEA algorithm is the result of these efforts.

The second part of the thesis was motivated by the demandingness of temperature measurements on the mould. Since the temperature is of principle importance for the Slush Moulding technology, there is a trend to replace the experimental temperature monitoring by a computer modelling of the corresponding temperature field. Therefore, we used the programme system ANSYS 15.0.7 to model the temperature field generated by the optimized positioning of the infrared heaters.

To conclude, we summarize the considerable findings and results.

1. The algorithm CDEA guarantees in general only convergence to a local minimum of the cost function. This phenomenon is caused by possible stagnation of the generations of the CDEA algorithm around a local minimum (premature convergence). This fact constitutes the principal weakness of CDEA. The result is demonstrated by a specific example of the cost function presented in full detail including the statistic data in Section 5.4.

2. This was the reason we looked for an improvement of the CDEA algorithm that would provide better results concerning the ability to identify the global minimum of the cost function. The MDEA algorithm is a result of these aspirations. The MDEA brings an essential improvement of the algorithm not only from theoretical but also from practical point of view.

3. The improved algorithm MDEA is not prone to the premature convergence because a certain ratio of random individuals in each generation makes it immune to the stagnation process. Besides, it is possible to prove that the algorithm MDEA converges asymptotically to the global minimum of the cost function in probabilistic sense (Section 5.6).

4. The role of random individuals in MDEA algorithm can be viewed from two different perspectives:

   - They eliminate the risk of premature convergence
   - In the long run they provide a random sampling of the search space of the given optimization task by random individuals

5. In case even MDEA algorithm stagnates and does not bring any improvement of the optimized minimum of the cost function, the random sampling

part of the algorithm can be used for quantitative estimates of the probability to find a state with a better cost function value. These results are the substance of Propositions 5.7.1 and 5.7.2.

6. When we suppose that the cost function is Lipschitz continuous we can use the results contained in Propositions 5.7.1 and 5.7.2 to estimate with a definite relative certainty the value of the cost function at the global minimum. This is the substance of Proposition 5.8.2.

7. In Chapter 6 we bring out the temperature field model used for the calculation of the temperature field in the mould. Since the temperature of the mould attains approximately 250 °C, the own heat radiation of the mould cannot be neglected.

8. Chapter 7 summarizes the practical task combining the optimization of the infrared heaters setting over the mould and the numerical modelling of the temperature field corresponding to the optimized heat flux. The temperature fields corresponding to the initial setting of heaters and to the optimized setting of heaters are presented. We also model the temperature field generated by fully uniform heat flux $47\,\mathrm{W/m^2}$ to have a comparison to the optimized positioning. The calculated results confirm that the temperature field generated by optimal positioning of infrared heaters is fully acceptable for the Slush Moulding technology.

From the practical point of view, the presented thesis brings a theoretically based and fully quantifiable method for infrared heaters positioning over the shell metal mould. Up to now, no other comparable technique has been available. Together with the temperature field modelling it brings a feasible contribution to the Slush Moulding technology.

On the other hand, unlike the infrared heating and temperature field modelling, the MDEA algorithm is a universal and efficient optimization tool. It can be tested and utilized in a wide range of optimization tasks with a very good prospective. The presented theoretical statements and conclusions concerning the MDEA algorithm have general validity and go far beyond the area of heat phenomena modelling.

# Bibliography

[1] *M. Affenzeller, S. Winkler, S. Wagner, A. Beham*: Genetic Algorithms and Genetic Programming. CRC Press, Boca Raton (2009).

[2] *R. Bartoszyński, M. Niewiadomska-Bugaj*: Probability and Statistical Inference. Wiley - Interscience, John Wiley & Sons, Inc., Publication, ISBN 978-0-471-69693-3 (2008).

[3] *A. Beiser*: Perspectives of Modern Physics. Academia, Prague (1978). (In Czech.)

[4] *Z. Beran*: Partial Differential Equations and Their Importance for Applications. Seminar Texts, Centre for Development of Advanced Control and Sensor Technologies, (2011). (In Czech.)

[5] *Y. A. Cengel, A. J. Ghajar*: Heat and Mass Transfer: Fundamentals and Applications. McGraw-Hill Education, New York (2015).

[6] *L. C. Evans*: Partial Differential Equation. Second Edition. Graduate Studies in Mathematics, Volume 19, America Mathematical Society, Providence, Rhode Island (2010).

[7] *M. Feistauer, K. Najzar*: Finite Element Approximation of a Problem with a Nonlinear Boundary Condition. Numer. Math., 78 (1998), pp. 403–425.

[8] *M. Feistauer, K. Najzar, K. Švadlenka*: On a Parabolic Problem with Nonlinear Newton Boundary Condition. Comment. Math. Univ. Carolin., 43 (2002), pp. 429–455.

[9] *J. Franců*: Monotone Operators. A Survey Dedicated to Applications to Differential Equations, Appl. Math., 35 (1990), pp. 257–301, .

[10] *Ch. Grossmann, H. G. Roos, M. Stynes*: Numerical Treatment of Partial Differential Equations, Springer-Verlag Berlin Heidelberg, ISBN 978-3-540-71582-5, (2007).

[11] *Z. Hu, S. Xiong, Q. Su, X. Zhang*: Sufficient Conditions for Global Convergence of Differential Evolution Algorithm. J. Appl. Math., Hindawi Publishing Corporation, Vol. 2013, pp. 14, http://dx.doi.org/10.1155/2013/193196.

[12] *R. Knobloch, J. Mlýnek, R. Srb*: Improving Convergence Properties of a Differential Evolution Algorithm. Proceedings of 42nd International Conference Applications of Mathematics in Engineering and Economics 2016, published by the American Institute of Physics, 1789, 030005 (2016), doi: 10.1063/1.4968451.

[13] *R. Knobloch, J. Mlýnek, R. Srb*: The Classic Differential Evolution Algorithm and Its Convergence Properties. Journal Applications of Mathematics Vol. 62 (2017), No. 2, published by Institute of Mathematics of the Czech Academy of Sciences, Prague, pp. 197–208, doi: 10.21136/AM.2017.0274-16.

[14] *R. Knobloch, J. Mlýnek, R. Srb*: Convergence Rate of the Modified Differential Evolution Algorithm. Proceedings of 43rd International Conference Applications of Mathematics in Engineering and Economics 2017, published by the American Institute for Physics, Conf. Proc. 1910, 030005-1-030005-8, ISBN 987-0-7354-1602-4, doi: 10.1063/1.5013964.

[15] *J. Královcová, J. Loufek*: Simulation of Radiative Heat Flux Distribution Under an Infrared Heat Emitter. Acta Polytechnica, Prague: Czech Technical University, Vol. 55 (2015), No. 1, pp. 22–28, ISSSN 1210-2709.

[16] *M. Křížek, L. Liu*: Finite Element Analysis of a Radiation Heat Transfer Problem. J. Comput. Math., 16 (1998), No. 4, pp. 327–336.

[17] *M. Křížek, L. Liu, P. Neittaanmäki*: Finite Element Analysis of a Nonlinear Elliptic Problem with a Pure Radiation Condition. Applied Nonlinear Analysis, Kluwer Academic/Plenum Publishers, New York, (1999), pp. 271–280.

[18] *M. Křížek, P. Neittaanmäki*: Finite Element Approximation of Variational Problems and Applications, Chapman and Hall, CRC Monographs and Surveys in Pure and Applied Mathematics, Longman Scientific & Technical, Harlow (1990).

[19] *M. Křížek, P. Neittaanmäki*: Mathematical and Numerical Modelling in Electrical Engineering, Theory and Applications, Kluwer Academic Publishers, Dordrecht, Boston, London (1996).

[20] *M. Křížek, K. Segeth*: Numerical Modelling of Problems in Electrical Engineering. Charles University in Prague, Karolinum Publishing, Prague (2001). (In Czech.)

[21] *Z. Michalewicz*: Genetic Algorithms + Data Structures = Evolution Programs. Springer-Verlag Berlin Heidelberg New York (1999).

[22] *J. Mlýnek, R. Knobloch*: The Model of Non-stationary Heat Conduction in a Metal Mould. In T. Březina, R. Jablonski (Eds.), Proceedings of the International Conference Mechatronics 2017, Recent Technological and Scientific Advances, Springer International Publishing AG (2018), ISBN 978-3-319-65959-6, ISBN 978-3-319-65960-2 (eBook), doi: 10.1007/978-3-319-65960-2.

[23] *J. Mlýnek, R. Knobloch*: Model of Shell Metal mould Heating in the Automotive Industry. J. Appl. Math, 63 (2018), pp. 111–124.

[24] *J. Mlýnek, R. Knobloch, R. Srb*: Optimization of a Heat Radiation Intensity and Temperature Field on the Mould Surface. Proceedings of $30^{th}$ European Conference on Modelling and Simulation, Regensburg, Germany, ISBN 987-0-9932440-2-5, doi: 10.7148/2016-0425.

[25] *J. Mlýnek, R. Knobloch, R. Srb*: Temperature Field Optimization on the Mould Surface. In: R. Jablonski, T. Březina (Eds.), Proceedings of the 11th International Conference Mechatronics 2015, Faculty of Mechatronics, Warsaw University of Technology, Warsaw (2015), Springer, 225–230, ISBN 987-3-319-23921-7, doi: 10.1007/978-3-319-23923-1-34.

[26] *J. Mlýnek, R. Knobloch, R. Srb*: Mathematical Model of the Metal Mould Temperature Optimization. Proceedings of the conference Applications of Mathematics in Engineering and Economics. Published by American Institute of Physics, Conference Proceedings 1690, 020018(2015), doi: 10.1063/1.4936696.

[27] *J. Mlýnek, R. Knobloch, R. Srb*: Use of a Differential Evolution Algorithm for the Optimization of the Heat Radiation Intensity. A contribution at the conference Applications of Mathematics 2015, organized by the Institute of Mathematics, Czech Academy of Sciences, 2015.

[28] *J. Mlýnek, R. Srb*: The process of an optimized heat radiation intensity calculation on a mould surface. Proc. of the 26th European Conference on Modelling and Simulation, pp. 461-467, May 2012, Koblenz, Germany, ISBN 978-0-9564944-4-3.

[29] *J. Mlýnek, R. Srb, R. Knobloch*: The Use of Graphics Card and nVidia CUDA Architecture in the Optimization of the Heat Radiation Intensity. In: J. Chleboun, P. Přikryl, K. Segeth, J. Šístek, T. Vejchodský (Eds.), Proc. of the Conference Programs and Algorithms of Numerical Mathematics 17, Institute

of Mathematics of the Czech Academy of Sciences, Prague (2014), 150–155, dml.cz/handle/10338.dmlcz/702677.

[30] *J. Mlýnek, T. Martinec, R. Srb*: Heating of Mould in Manufacture of Artificial Leathers in Automotive Industry. Proceedings of the 10th International Conference Mechatronics 2013, Editors T. Březina, R. Jabloński, Springer, October 2013, pp. 119–126, ISBN 978-3-319-02293-2.

[31] *J. Mlýnek, A. Potěšil*: Radiation Heating, Theory and Industrial Practice. Technical University in Liberec, Faculty of Mechatronics, Informatics and Interdisciplinary Studies, Lenam, Department of Calculations, Simulations and Analyses, ISBN 978-80-7372-884-7, Liberec (2012). (In Czech.)

[32] *J. Nečas*: Direct Methods in the Theory of Elliptic Equations. Springer-Verlag, Berlin, Heidelberg (2012).

[33] *A. Potěšil, M. Hušek*: Criterion of Optimal Infra-heating of Moulds in Production of Artificial Leathers. In Proceedings of 50th International Conference EAN 2012, Tábor, The Czech Republic, 6 – 9 June 2011, pp. 345-352. ISBN 978-80-01-05060-6.

[34] *K. V. Price:* Differential Evolution: A Fast and Simple Numerical Optimizer, NAFIPS 1996, pp. 524-527.

[35] *K. V. Price, R. M. Storn, J. A. Lampien*: Differential Evolution – A Practical Approach to Global Optimization. Springer-Verlag, Berlin, Heidelberg (2005).

[36] *K. Rektorys*: Variational Methods in Mathematics, Science and Engineering. Second Edition, Academia, Prague (1999). (In Czech.)

[37] *K. Rektorys*: The Method of Discretization in Time and Partial Differential Equations. SNTL - Technical Literature Publishing, Prague (1985). (In Czech.)

[38] *L. Schwartz*: Mathematical Methods in Physics. SNTL - Technical Literature Publishing, Prague (1972). (In Czech.)

[39] *D. Simon*: Evolutionary Optimization Algorithms. John Wiley & Sons, Hoboken, New Jersey (2013).

[40] *J. J. Stocker*: Differential Geometry. John Wiley & Sons, New York (1989).

[41] *R. M. Storn, K. V. Price:* Differential Evolution - A Simple and Efficient Heuristics for Global Optimization over Continuous Spaces. Journal of Global Optimization 11, Kluwer Academic Publishers (1997), pp. 341–359.

[42] *A. Štrba*: Optics, General Physics 3. Technical Literature Publishing, Prague (1979). (In Slovak.)

[43] *E. Zeidler:* Applied Functional Analysis, Applications to Mathematical Physics. Applied Mathematical Sciences 108, Springer-Verlag, New York Berlin Heidelberg Inc., ISBN 0-387-94442-7, (1999).

[44] *E. Zeidler:* Nonlinear Functional Analysis and Its Applications I, Fixed Point Theorems. Springer-Verlag, New York Berlin Heidelberg Inc., ISBN 0-387-90914-1, (1993).

[45] *E. Zeidler:* Nonlinear Functional Analysis and Its Applications II/A, Linear Monotone Operators. Springer-Verlag, New York, Berlin, Heidelberg Inc., ISBN 0-387-96802-4 (1990).

[46] *E. Zeidler:* Nonlinear Functional Analysis and Its Applications II/B, Nonlinear Monotone Operators. Springer-Verlag, New York, Berlin, Heidelberg Inc., ISBN 0-387-97167-X (1990).

[47] *E. Zeidler:* Nonlinear Functional Analysis and Its Applications III, Variational Methods and Optimization. Springer-Verlag, New York Berlin Heidelberg Tokyo Inc., ISBN 0-387-90915-X (1985).

[48] *E. Zeidler:* Nonlinear Functional Analysis and Its Applications IV, Applications to Mathematical Physics. Springer-Verlag, New York, Berlin, Heidelberg Inc., ISBN 0-387-96499-1 (1997).

[49] *J. Zhang, A. C. Sanderson*: Adaptive Differential Evolution. Springer-Verlag, Berlin, Heidelberg (2009).

[50] *K. Zvára, J. Štěpán*: Probability and Mathematical Statistics. Matfyzpress, Prague (2012). (In Czech.)